PERGAMON

Vision Research 40 (2000) 2307–2327

Vision Research

www.elsevier.com/locate/visres

Detecting disorder in spatial vision

Dennis M. Levi [a,*], Stanley A. Klein [b], Vineeta Sharma [a,1], Lisa Nguyen [a]

[a] *University of Houston, College of Optometry, Houston, TX 77204-6052, USA*
[b] *University of California, Berkeley, School of Optometry, Berkeley, CA 94720, USA*

Received 27 July 1999; received in revised form 19 January 2000

Abstract

In normal foveal vision, visual space is accurately mapped from retina to cortex. However, the normal periphery, and the central field of strabismic amblyopes have elevated position discrimination thresholds, which have often been ascribed to increased 'intrinsic' spatial disorder. In the present study we evaluated the sensitivity of the human visual system (both normal and amblyopic) to spatial disorder, and asked whether there is increased 'intrinsic' topographical disorder in the amblyopic visual system. Specifically, we measured thresholds for detecting disorder (two-dimensional Gaussian position perturbations) either in a horizontal string of N equally spaced samples (Gabor patches), or in a ring of equally spaced samples over a wide range of feature separations. We also estimated both the 'equivalent intrinsic spatial disorder' and sampling efficiency using an equivalent noise approach. Our results suggest that both thresholds for detecting disorder, and equivalent intrinsic disorder depend strongly on separation, and are modestly increased in strabismic amblyopes. Strabismic amblyopes also show markedly reduced sampling efficiency. However, neither amblyopic nor peripheral vision performs like ideal or human observers with added separation-independent positional noise. Rather, the strong separation dependence suggests that the 'equivalent intrinsic disorder' may not reflect topographic disorder at all, but rather may reflect an abnormality in the amblyopes' Weber relationship. © 2000 Elsevier Science Ltd. All rights reserved.

Keywords: Spatial vision; Amblyopes; Disorder

1. Introduction

In normal foveal vision, visual space is accurately mapped from retina to cortex. The precise topographical mapping provides a veridical representation of the world, and enables the visual system to maintain very precise spatial order. Thus, in normal foveal vision, we are able to judge the locations of objects with great precision when a reference is nearby.

Not all visual systems are able to judge location so accurately. For example, both the normal periphery, and the central field of strabismic amblyopes have elevated position discrimination thresholds. This poor positional discrimination has often been ascribed to increased 'intrinsic' spatial disorder, i.e. topographical disorder in the positions of cortical receptive fields, that is uncalibrated (Hess, Campbell & Greenhalgh, 1978; Levi & Klein, 1985; Levi, Klein & Aitsebaomo, 1985; Wilson, 1991; Hess & Field, 1993, 1994; Field & Hess, 1996; Wang, Levi & Klein, 1998).

Evidence for raised intrinsic spatial disorder comes primarily from equivalent noise (or perturbation) studies. This approach has been widely used to estimate equivalent noise both in normal (Barlow, 1956; Levi & Klein, 1990a; Pelli, 1990) and amblyopic vision (Watt & Hess, 1987; Levi & Klein, 1990b; Kiorpes, Kiper & Movshon, 1994; Wang et al., 1998). Specifically, performance is measured in the presence of external noise, and the amount of external noise that raises thresholds by a criterion amount (generally $\sqrt{2}$) is taken as an estimate of the equivalent intrinsic noise. Several studies have used this approach to measure position thresholds in the presence of noise (positional jitter), and have concluded that amblyopic eyes have increased equivalent positional noise (and hence increased topographical disorder). However, this interpretation is open to question. For one thing, several studies (Watt & Hess, 1987; Wang et al., 1998) used broadband

* Corresponding author. Fax: +1-713-7431888.
E-mail address: dlevi@uh.edu (D.M. Levi).
[1] Present address: Alcon Laboratories, Fort Worth, Texas.

0042-6989/00/$ - see front matter © 2000 Elsevier Science Ltd. All rights reserved.
PII: S0042-6989(00)00087-0

stimuli (lines). Amblyopic eyes analyze broadband stimuli through lower spatial frequency filters, so the increased 'equivalent noise' might actually reflect alterations in filter size, rather than increased topographical disorder in the brain (Levi, Waugh & Beard, 1994). Recently, Hess, McIlhagga and Field (1997) addressed this issue by using narrow-band (Gabor) stimuli. They found that amblyopic eyes indeed required higher amounts of external noise to produce a threshold elevation than did fellow eyes, and that adding this external noise to the non-amblyopic eye mimics the amblyopic eye's performance on a task involving path detection (i.e. finding a path defined by Gabor orientation among distracters). They argued that the amblyopic eye's performance is limited by the intrinsic topographical disorder of cortical receptive fields, which is not calibrated, and that this disorder can be so extreme that it can actually exceed the receptive field size (Hess & Field, 1994; Field & Hess, 1996; but see also Levi & Klein, 1996). Further, Hess and his colleagues (Hess & Holliday, 1992; Demanins & Hess, 1996; Hess, Wang, Demanins, Wilkinson & Wilson 1999) have argued that the positional deficit is 'scale invariant', suggesting that the cortical topology is disrupted similarly over a wide range of spatially scaled neural maps. Since amblyopia is often considered a 'high spatial frequency deficit' (e.g. Hess & Howell, 1977; Levi & Harwerth, 1977; Bradley & Freeman, 1981), this is a surprising result.

On the other hand, some pattern discrimination tasks are robust to positional disorder, and the tolerance to positional jitter is determined mainly by feature separation, both in normal and amblyopic vision (Levi, Sharma & Klein, 1997; Levi, Klein & Sharma, 1999; Levi & Klein, 2000). Specifically, both normal observers and strabismic amblyopes are able to discern the orientation of an E-like figure when the features are subjected to positional disorder with a standard deviation of up to about half the separation of the features (Levi et al., 1997, 1999). Moreover, strabismic amblyopes seem to be inefficient in using all of the stimulus samples for pattern discrimination (Wang et al., 1998; Levi et al., 1999). Thus, our goal in the present paper was to evaluate the sensitivity of the human visual system (both normal and amblyopic) to spatial disorder, and to ask whether there is increased 'intrinsic' topographical disorder in the amblyopic visual system. Thus, in the present manuscript, we measured thresholds for detecting disorder (two-dimensional Gaussian position perturbations) either in a horizontal string of N equally spaced samples (Gabor patches), or in a ring of equally spaced samples over a wide range of feature separations. We also estimated both the equivalent intrinsic spatial disorder and the sampling efficiency using the equivalent noise approach that has been widely used to estimate equivalent noise both in normal (e.g. Barlow, 1956; Pelli, 1990) and amblyopic vision. Our results suggest that both thresholds for detecting disorder, and equivalent intrinsic disorder depend strongly on separation, and are only modestly increased in strabismic amblyopes. Moreover, we show that neither amblyopic nor peripheral vision performs like ideal or human observers with added positional noise. Rather, the strong separation dependence suggests that the 'equivalent intrinsic disorder' may not reflect topographic disorder at all, but rather may reflect an abnormality in the comparison process that leads to Weber's law in the amblyopic visual system. On the otherhand, sampling efficiency seems to be quite robust to stimulus conditions, and markedly reduced in some amblyopes.

2. Methods

The stimulus consisted of either a string (Fig. 1 top) or a ring (Fig. 1 bottom) of N equally spaced circular Gabor patches (i.e. the luminance distribution of each element is described by the product of a circular Gaussian and an oriented sinusoid). We used Gabor patches because they are limited in their spatial frequency bandwidth (we used several different bandwidths, as specified in the text). The use of band-limited stimuli make it unlikely that differences between normal and amblyopic eyes can be explained on the basis of shifts toward lower spatial frequency linear first stage filters when viewing with the amblyopic eye (Levi et al., 1994). Unless otherwise specified, the sinusoidal carrier was always vertical and in sine phase.

The stimuli were displayed on either a Mitsubishi Diamond Scan 20H or a 21TX monitor via a Cambridge Research Systems VSG 2 graphics card. The monitor frame rate was 72 Hz (non-interlaced) and the mean luminance of the display area was 56 cd/m^2.

In order to evaluate the sensitivity to spatial disorder, we measured thresholds for disorder detection using a 2-interval forced-choice (2-IFC) procedure. Rather than using deterministic position shifts, we created spatial disorder by perturbing the positions of the samples using two-dimensional Gaussian position jitter. Two-dimensional Gaussian jitter might be expected to mimic the topological disorder in human cortical receptive fields. The Appendix shows the connection between the disorder thresholds for 2-D Gaussian jitter (i.e. direction unknown) and the thresholds obtained for deterministic offsets (i.e. direction known) which are usually obtained for Vernier alignment or bisection. In the string experiments, one interval contained a horizontal string consisting of N equally spaced, parallel patches and the other contained the same patches, with their positions independently perturbed by one of five magnitudes of two-dimensional Gaussian jitter (specified by

the standard deviation (SD) and presented at random). Unless otherwise specified, the carrier was always vertical, orthogonal to the horizontal orientation of the string, so that it would not provide a useful cue for alignment, and N was 5. The observer's task was to decide which interval contained the jitter. In order to evaluate performance over a wide range of stimulus conditions, we used two different strategies: (1) varying the observers' viewing distance, while keeping the screen dimensions of the stimuli constant. This has the advantage that at each viewing distance, the stimuli were scaled replicas. However, it has the disadvantage that changes in patch size, spatial frequency and separation are inextricably correlated. Thus we also (2) fixed the observer's viewing distance, patch size and spatial frequency, and varied the separation of the patches on the screen.

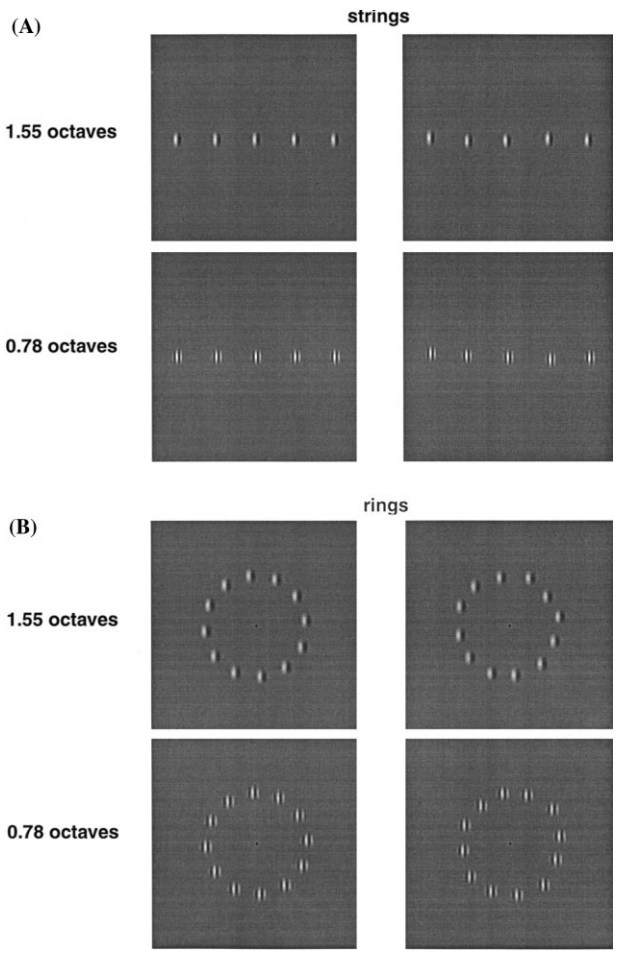

Fig. 1. Examples of the stimuli. Top 4 panels: strings; the lower 4 panels: rings. (A) Examples of strings of five Gabor patches (with vertical carriers) with no disorder (left panels) or disorder of approximately 3% of the inter-patch separation (right panels). (B) Examples of rings of N Gabor patches (with vertical carriers) with no disorder (left panels) or disorder of 5% of the inter-patch separation (right panels). For both strings and rings the top two panels have a 1.55 octave bandwidth; the lower two panels have a 0.78 octave bandwidth.

In the *ring* experiments, one interval contained N patches arranged (with uniform separation) around a notional circle with a fixed radius (R). In the other interval (chosen at random) the sample positions were independently perturbed by two-dimensional Gaussian jitter (as in the string experiments). For the ring experiments a black square (0.05°) was constantly present at the center of the screen to ensure appropriate fixation. To ensure that the fixation target did not provide a useful cue for shape discrimination, the actual positions of all of the samples varied randomly (by varying the position on the ring of the 'first' sample). In addition, the location of the entire ring was randomly offset from the center, by a uniform jitter (approximately twice the threshold) independently in one of eight orientations (at 45° intervals). In order to vary the separation of the patches we either varied the viewing distance (this varies the ring radius, patch size and spatial frequency as well as the interpatch separation), or varied N (the number of patches around a ring of fixed radius). This method results in a fixed patch size, spatial frequency and radius. These two rather different methods give similar results when thresholds are specified relative to the interpatch separation (Levi & Klein, 2000).

For both the string and the ring, each of the two temporal intervals was 500 ms (signaled by two tones) with an interstimulus interval of 500 ms, and the observer's task was to report which interval contained the disordered stimulus. Auditory feedback was provided after each response. Psychometric curves (with five near-threshold perturbations) were obtained for each stimulus condition, and disorder thresholds were estimated using a Weibull function. The disorder detection thresholds presented in Section 3 section refer to the means of at least four individual threshold estimates, and are specified at 75% correct ($d' \approx 1.0$).

In some experiments we equated stimulus visibility in the two eyes of our observers. This was accomplished by measuring detection thresholds (using a two-alternative forced choice procedure) for a single patch either at fixation, or at the position of one of the adjacent patches of the string or on the radius of the ring. These detection thresholds were used to equate performance in the two eyes (in multiples of the detection threshold).

2.1. Observers

Four observers with normal visual acuity (three of the authors, and one naive as to the purpose of the experiments) and seven observers with strabismic amblyopia (see Table 1 for details) served as observers. For all observers, viewing was monocular, with the untested eye occluded with a black patch. All observers were well practiced in making psychophysical judgments.

Table 1
Visual characteristics of amblyopic observers

Observer	Age	Sex	Eye	Rx.	Acuity[a]	Fixation[b]	Strabismus
RH	32	M	O.D.	$-1.00/-0.50\times170$	20/15	Central	
			O.S.	$-1.50/-1.50\times10$	20/59	Unsteady	Microtropia l. et., 2Δ
JB	39	M	O.D.	$+1.75/-0.50\times142$	20/49	0.25° nasal	Constant r. et., 6Δ
			O.S.	$+1.25/-1.0\times025$	20/20	Central	
QM	18	M	O.D.	-0.75	20/20	Central	
			O.S.	$+2.25/-2.75\times155$	20/60	3° nasal	Constant l. et., 7Δ
DM	39	F	O.D.	$-0.50/-0.25\times92$	20/20	Central	
			O.S.	$+2.50/-1.0\times160$	20/80	0.50° nasal	Constant l. xt., 3Δ
DS	25	M	O.D.	$+2.25$	20/30	2° nasal	Constant r. et. 8Δ
			O.S.	$+0.50$	20/20	Central	
CB	37	M	O.D.	$+4.25$	20/15	Central	
			O.S.	$-9.75/-0.75\times140$	20/200	0.75–1° nasal	Constant l. et., 4Δ
AJ	27	F	O.D.	$+5.50/-2.50\times20$	20/60	1.5° temporal	Constant r. xt., 4Δ
			O.S.	-0.25	20/15	Central	

[a] 75% correct on Davidson–Eskridge charts.
[b] Fixation determined with Haidinger's brushes and visuoscopy.

3. Results

The results are presented in two sections: we first consider the detection of disorder (with no added jitter), and then in subsequent sections we consider performance with added jitter.

3.1. Section 1

3.1.1. Detecting disorder in strings

In normal foveal vision, thresholds for detecting disorder depend strongly on the separation of the features (Fig. 2). Varying the observer's viewing distance while fixing the stimulus on the screen (i.e. varying the 'spatial scale' (Hess & Holliday, 1992) — Fig. 2 top panel) changes the patch separation, carrier spatial period and envelope standard deviation in inverse proportion to the viewing distance. However, for normal observers, holding the viewing distance, carrier spatial period and envelope standard deviation fixed, and varying the patch separation on the screen gives essentially identical results (as can be seen by comparing the 'vary distance' and 'vary separation' data in Fig. 2 bottom panel). Note that Fig. 2 (bottom panel) presents data from a variety of different stimulus conditions (SD, SF, etc.) showing that in normal foveal vision the stimulus details make very little difference to performance. The dotted line shows the prediction of a simple eccentricity-based model (Levi & Tripathy, 1996) in which threshold, $\mathrm{Th} = k(\mathrm{Ecc} + E_2)$ (where k is a fraction [$\approx 1/70$] of the effective eccentricity, $(\mathrm{Ecc} + E_2)$ of the patches on each side of the central patch; Ecc is the patch eccentricity and E_2 is the eccentricity at which the threshold is twice the foveal threshold).

All amblyopic eyes showed increased thresholds for detecting disorder as compared to the non-amblyopic eyes (Figs. 3 and 4), and the increased thresholds are most evident at small separations and/or high spatial frequencies. With the exception of CB (the most severe amblyope — Fig. 3A) and QM (Fig. 3B) all observers showed normal or near normal thresholds at large separations. For the amblyopic eyes both separation and carrier spatial frequency can influence performance. Low stimulus visibility may contribute to the loss at high spatial frequencies; however, disorder thresholds are increased in the amblyopic eye even when the visibility is matched to that of the non-amblyopic eye (by lowering the contrast in the non-amblyopic eye — gray symbols labeled 'Eq Visi' in Fig. 4A). The amblyopic loss increases at high spatial frequencies (for a fixed patch size and separation) even when the stimulus visibility is held constant (Fig. 4B). It is interesting to note that the effect of contrast on performance is similar in the two eyes (when specified with respect to the stimulus visibility in contrast threshold units (CTU) — Fig. 4C).

One difficulty with the strings (or for that matter with 3-patch alignment or bisection) is that varying the separation of the patches (by varying the viewing distance or varying only the patch separation) alters the eccentricity of the non-central patches. Thus, patch separation and eccentricity are confounded. Indeed, the central assumption of the eccentricity model (dotted line in Fig. 2) is that performance is primarily limited by the eccentricity of the patches on either side of the middle patch. Thus, it is not clear whether most amblyopes normalize at large separations because the patches that limit performance are more eccentric, or because of the separation per se. For this reason we also measured the detection of disorder in rings.

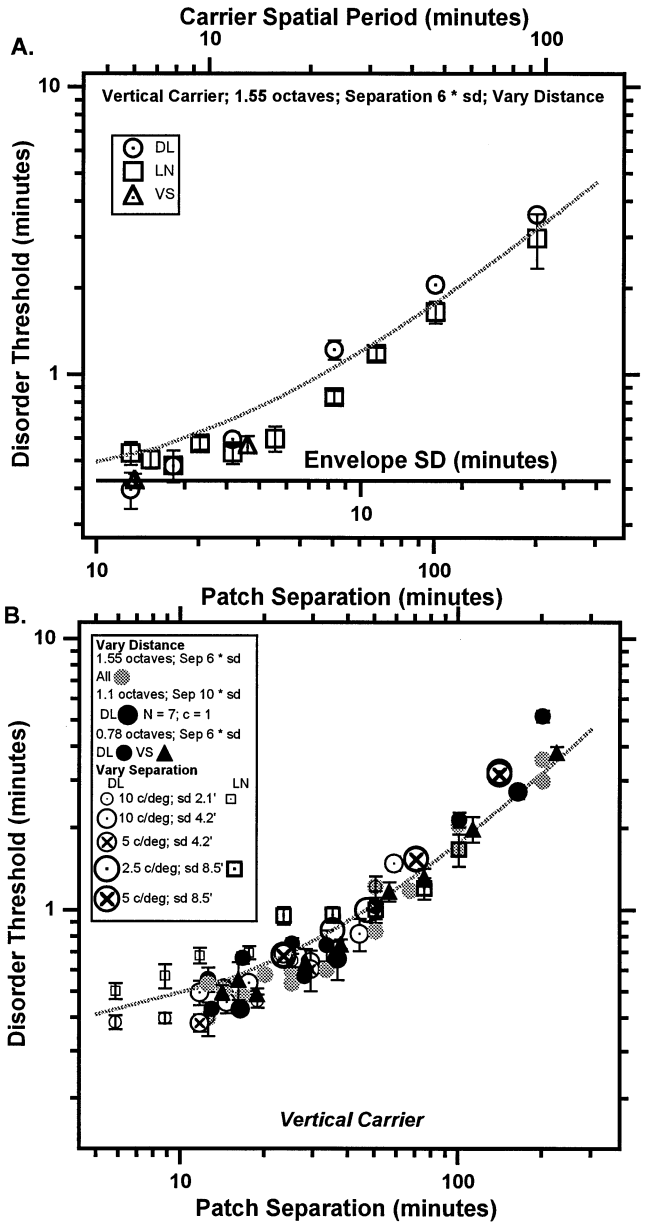

Fig. 2. Thresholds for detecting disorder in strings depend strongly on the separation of the features in normal foveal vision. Thresholds were obtained by: (A) varying the observer's viewing distance while fixing the stimulus on the screen. This increases the patch separation (bottom abscissa), carrier spatial period (top abscissa), and envelope standard deviation (middle abscissa), in inverse proportion to the viewing distance. Data are shown for three normal observers with a stimulus bandwidth of 1.55 octaves and a vertical carrier. (B) holding the viewing distance, carrier spatial period and envelope standard deviation fixed, and varying the patch separation on the screen (open symbols). 'Vary separation' data are shown for two observers and various carrier spatial frequencies and envelope standard deviations. For comparison the gray symbols show the 'vary distance' data from Fig. 2A, and the filled symbols show vary distance data for other bandwidths and numbers of patches. The dotted line (in A and B) shows the prediction of a simple eccentricity-based model (see text for details) in which threshold is limited by the eccentricity of the patches on each side of the central patch.

3.1.2. Detecting disorder in rings

In normal foveal vision, thresholds for detecting disorder in rings comprised of 12 patches also depend strongly on the separation of the features (Fig. 5). Varying the observer's viewing distance while fixing the stimulus on the screen increases the ring radius, the inter-patch separation, carrier spatial period and envelope standard deviation in inverse proportion to the viewing distance. However, for normal observers, holding the viewing distance, carrier spatial period and envelope standard deviation fixed, and varying the patch separation by altering the ring radius on the screen (circles with crosses in Fig. 5) gives essentially identical results. Elsewhere (Keeble & Hess, 1999; Levi & Klein, 2000) separation has been shown to be the principal limiting factor for rings. Similar to the string results, amblyopic eyes perform more or less normally at large separations and low spatial frequencies (filled symbols), and are degraded at small separations and low spatial frequencies. Varying only the carrier spatial frequency (while holding the circle radius and envelope standard deviation constant) has a modest effect on normal (or non-amblyopic) eyes (see also Keeble & Hess, 1999); however it has a marked effect on the amblyopic eyes (Fig. 6). For example, for DM's amblyopic eye, the disorder threshold was about one log unit greater than that of the non-amblyopic eye at 9 c/deg, and RH was unable to perform the task with his amblyopic eye at spatial frequencies above 12 c/deg. This amblyopic loss is not simply a matter of reduced visibility. Reducing the contrast in the non-amblyopic eye to equate the patch visibility (in multiples of the contrast detection threshold (ctu) gray squares) to that of the amblyopic eye at 100% contrast, does not equate performance in the two eyes; however, the small effect of spatial frequency on the normal and non-amblyopic eyes may be at least in part due to reduced visibility of the patches.

3.1.3. Detection of disorder is a Weber fraction of separation

For both strings and rings, disorder detection thresholds follow Weber's law, i.e. they are roughly proportional to the separation between patches. For strings (Fig. 7) the Weber fractions of normal observers (crosses) decrease (improve) to approximately 0.02 (1/50) as separation increases up to 30 min. For strings, varying the separation between patches also alters the eccentricity of the outer patches from the central (fixated) patch. As noted above, for strings, performance is reasonably well predicted by the eccentricity of the patches adjacent to the central patch (as shown below, only three or four equally spaced patches contribute to performance with strings — Fig. 14A,B). The Appendix shows that the Weber fraction of around 0.02 (1/50) is just what would be expected for disorder

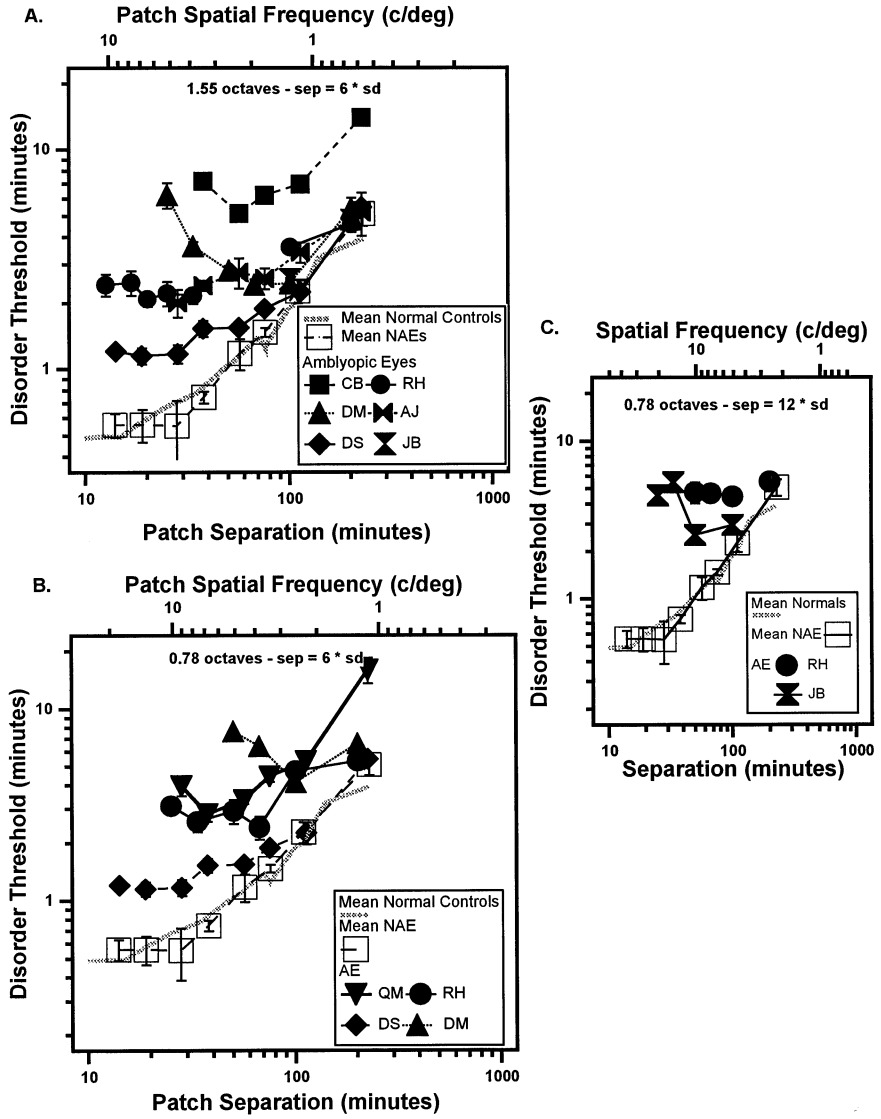

Fig. 3. Thresholds for detecting disorder in strings depend strongly on the separation of the features in amblyopic vision. Thresholds were obtained by varying the observer's viewing distance while fixing the stimulus on the screen. (A) Data are shown for the amblyopic eyes of six strabismic amblyopes (solid symbols) with a stimulus bandwidth of 1.55 octaves and a vertical carrier. The patch separation was always six times the standard deviation. The open squares are mean data of all the non-amblyopic eyes, and the dotted line is the mean data of the three normal control observers over all conditions. (B) Data are shown for the amblyopic eyes of four strabismic amblyopes (solid symbols) with a stimulus bandwidth of 0.78 octaves and a vertical carrier. The patch separation was always six times the standard deviation. Other details as in (A). (C) Data are shown for the amblyopic eyes of two strabismic amblyopes (solid symbols) with a stimulus bandwidth of 0.78 octaves and a vertical carrier. The patch separation was always 12 times the standard deviation. Other details as in (A).

detection (with direction of offset unknown), based on studies of alignment and bisection with direction of offset known.

Interestingly, for rings (Fig. 8), thresholds (specified as Weber fractions) of the normal and non-amblyopic eyes are essentially identical when varying the viewing distance (and thus the radius, patch size and spatial frequency — Fig. 8A) or when fixing the viewing distance and varying the separation by varying N (Fig. 8B) from $N = 3$ to 24. If separation is a critical determinant of the performance for rings, then varying N (the number of patches) while keeping the radius constant should result in a proportional change in thresholds, and thus a more or less constant Weber fraction for both normal and amblyopic eyes. This is strong evidence that patch separation constrains performance. Using different methods and observers we have previously reported that radius and N can be traded-off, indicating that it is the patch separation and not the eccentricity (which varies with radius) that constrains performance with rings (Levi & Klein, 2000).

The separation/eccentricity dependence of the amblyopic loss can be readily seen when plotted as a Weber fraction (Figs. — strings; Fig. 8 — rings). As noted

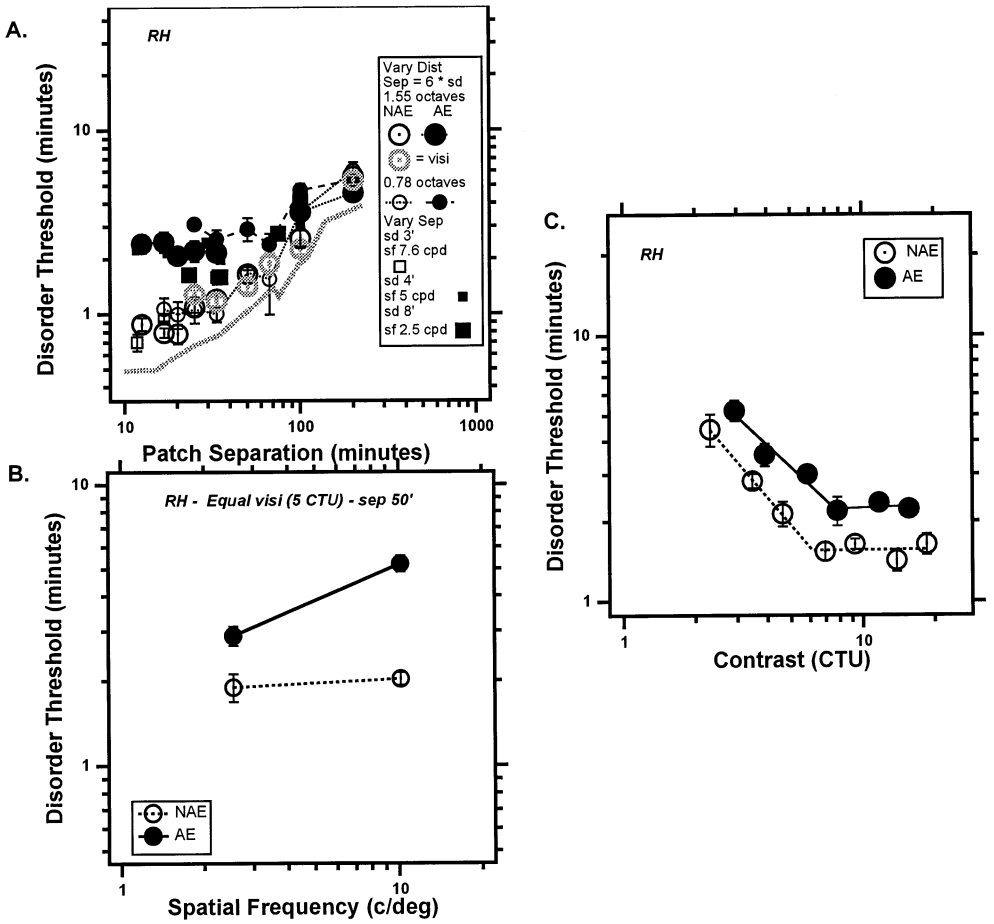

Fig. 4. Thresholds for detecting disorder in strings. (A) Each panel shows data for the amblyopic (solid symbols) and non-amblyopic (open symbols) of RH under a variety of conditions in which separation ('vary sep') or viewing distance ('vary dist') were varied. For the non-amblyopic eye, like the normal observers, performance shows little dependence on stimulus conditions (compare the vary distance and vary separation data). The amblyopic eyes demonstrates more pronounced effects of stimulus conditions. The gray symbols labelled ' = visi' show the performance of the non-amblyopic eye when the visibility is matched to that of the amblyopic eye (by lowering the contrast in the non-amblyopic eye). (B) For patches fixed in size and separation, the amblyopic loss increases at high spatial frequencies even when the stimulus visibility is held constant (the contrast of the patches was five times threshold for each eye and condition). (C) The effect of contrast on performance is similar in the two eyes (when specified with respect to the stimulus visibility in contrast threshold units (CTU)).

above, varying separation by altering the viewing distance changes both the separation and eccentricity of the patches (for both strings and rings). Under these conditions, the amblyopic loss is always clearly greatest at small separations/eccentricities (Figs. 7 and 8A), and only two observers show a loss at the largest patch separation (CB and QM Fig. 7). Reducing the contrast in the non-amblyopic eye to equate visibility accounts for some (but not all) of this loss (gray open symbols and see Figs. 4 and 6).

It is not clear from Figs. 7 and 8A whether the normalization at large separation/eccentricity is an effect of separation or eccentricity. Demanins and Hess (1996) found that 3-patch alignment thresholds normalize in some (but not all) amblyopic eyes, when the entire display is viewed peripherally. Varying the separation of the patches in a ring by varying N provides a direct test of the separation dependence with the patches at a fixed eccentricity (determined by the ring radius). Fig. 8B shows data for three strabismic amblyopes: DS, the mildest, shows slightly greater than a 2-fold loss at small separations, which normalizes by a separation of 60′. On the other hand, the other two observers show losses which are either more or less independent of separation, or actually increase with patch separation (or reduced N, e.g. RH). Note the rightmost datum for RH's amblyopic eye is dramatically elevated when compared to the rest of the data. This is for $N = 3$ where the task becomes one of judging whether a randomly oriented triangle is equilateral. We repeated this condition many times and do not understand why his amblyopic eye is so much poorer than the non-amblyopic eye in this condition.

3.2. Section 2

3.2.1. Estimating equivalent 'intrinsic' disorder and efficiency

Disorder thresholds are elevated in the amblyopic eyes of strabismic amblyopes, particularly at small separations and high spatial frequencies. One hypothesis is that thresholds are elevated because of increased 'intrinsic' topographical disorder in the visual cortex, which is uncalibrated (Hess & Field, 1993, 1994; Field & Hess, 1996). We have estimated the equivalent 'intrinsic' disorder, D_{eq}, using a perturbation paradigm. D_{eq} represents the amount of internal equivalent noise (disorder) added to the stimulus patches that would account for the observer's disorder detection threshold without any added external noise. This approach has been widely used to understand the limits of normal (e.g. Barlow, 1956; Zeevi & Mangoubi, 1984; Watt, Ward & Casco, 1987; Pelli, 1990; Levi & Klein 1990a) and amblyopic vision (e.g. Watt & Hess, 1987; Levi & Klein, 1990b; Kiorpes et al., 1994; Wang et al., 1998).

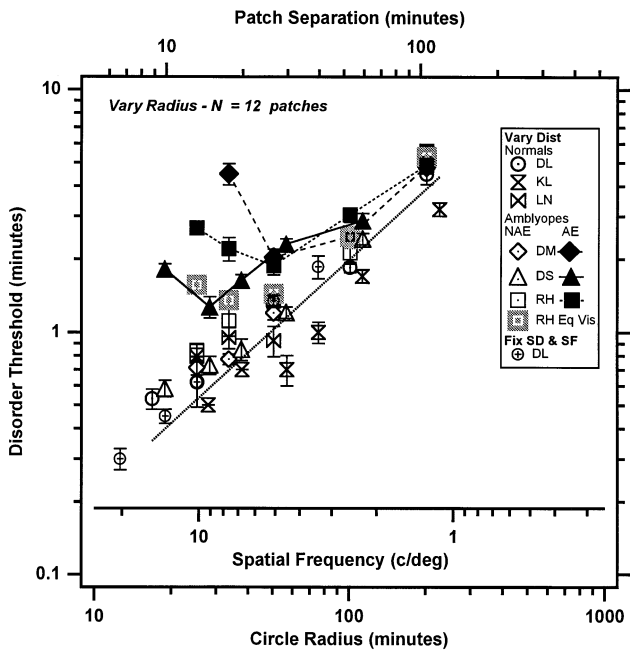

Fig. 5. Thresholds for detecting disorder in rings comprised of 12 patches. Disorder thresholds in rings also depend strongly on the separation (top abscissa) of the features in both normal (open symbols) and amblyopic eyes (solid symbols). Decreasing the observer's viewing distance while fixing the stimulus on the screen also increases the ring radius (lower abscissa), and envelope standard deviation, and decreases the carrier spatial frequency (middle abscissa) in inverse proportion to the viewing distance. Data are shown for three normal observers. For normal observer DL, holding the viewing distance, carrier spatial period and envelope standard deviation fixed, and varying the patch separation by altering the ring radius on the screen (circles with crosses) gives essentially identical results. Data are also shown for each eye of three amblyopes. Equating the stimulus visibility of the two eyes by lowering the contrast in the non-amblyopic eye (RH — gray square labeled 'Eq Vis') does not fully account for the amblyopic loss.

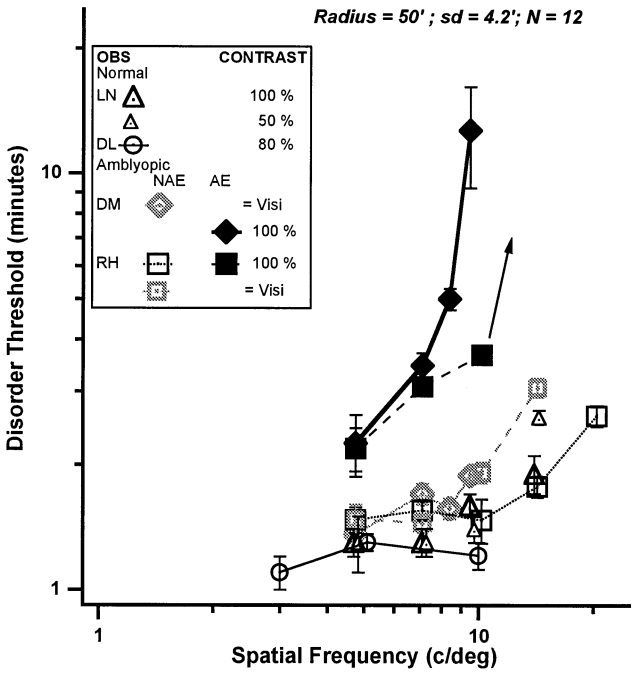

Fig. 6. Varying only the carrier spatial frequency (while holding the circle radius and envelope standard deviation constant) has a modest effect on normal (or non-amblyopic) eyes (open symbols); however it has a marked effect on the amblyopic eyes (solid symbols). This effect is not simply a matter of reduced visibility. Reducing the contrast in the non-amblyopic eye to equate the patch visibility (gray squares) does not equate performance in the two eyes.

Equivalent disorder can be estimated by fitting the data with a function of the form:

$$\mathrm{Th} = ((D_{eq}^2 + D_{ext}^2)/(N_{eff} - 1))^{1/2} \quad (1)$$

where N_{eff} refers to the effective number of samples used by the observer. The rationale for the factors $(N-1)^{1/2}$ rather than $(N)^{1/2}$ or $(N-2)^{1/2}$ is discussed in the Appendix. D_{eq} is the equivalent intrinsic disorder (i.e. the horizontal position of the knee in the function) and D_{ext} is the standard deviation of the external base disorder (2-D jitter).

Efficiency (E) is the ratio:

$$E = (N_{eff} - 1)/(N_{stim} - 1) \quad (2)$$

where N_{stim} is the number of samples in the stimulus. Our previous work suggests that amblyopic vision shows a loss of efficiency (i.e. that observers are unable to use multiple samples to reduce the effect of jitter [Wang et al., 1998; Levi et al., 1999]). This model is based on the assumption that the visual system has an internal error that acts like two-dimensional Gaussian position disorder (or jitter $- D_{eq}$). When the external jitter is small, it has little influence upon disorder thresholds; however, when it exceeds D_{eq}, then threshold is proportional to the external base jitter. Thus the parameter D_{eq} has frequently been taken to represent an estimate of the intrinsic error in the visual

system (see, e.g. Pelli, 1990). Here we use it to quantify the equivalent disorder.

Alternatively, D_{eq} can be replaced by Th_0 in Eq. (1) to give:

$$Th = (Th_0^2 + D_{ext}^2/(N_{eff} - 1))^{1/2} \quad (3)$$

where $Th_0 = D_{eq}(N_{eff} - 1)^{1/2}$. Th_0 is the disorder threshold for a stimulus with no external noise (i.e. the asymptotic threshold).

For an ideal observer $N_{eff} = N_{stim}$. $N - 1$ is present in these equations because a minimum of two samples are needed for detection of disorder.

We estimated both D_{eq} and E for our observers by measuring disorder discrimination thresholds for strings and rings with added two-dimensional Gaussian jitter and fitting the results with Eq. (1) (for D_{eq}) and Eq. (3) for (Th_0 and E) in normal observers (Fig. 9A,B — strings and Fig. 9C,D — rings) and in amblyopes (under conditions where the amblyopic eye shows elevated thresholds (Fig. 10 — strings and Fig. 11 — rings)). Table 2 summarizes the results for each of our observers.

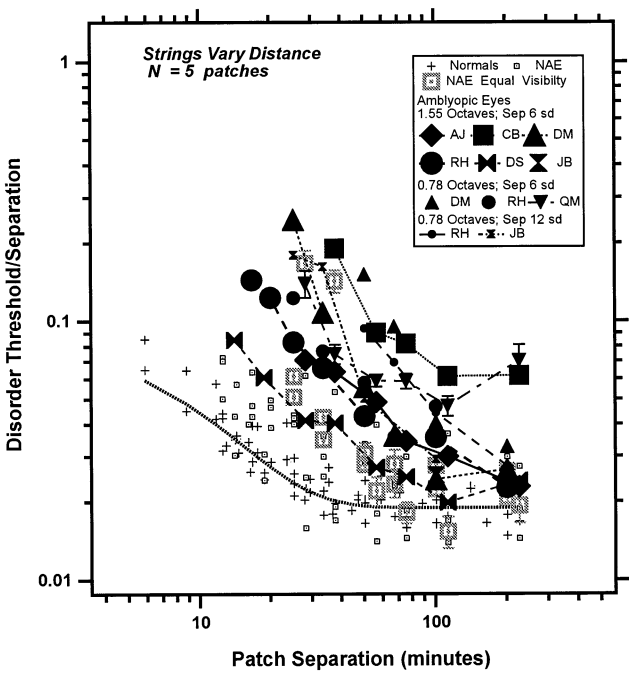

Fig. 7. Disorder detection thresholds for strings plotted as a Weber fraction of separation. The crosses are all of the 'vary distance' data of the normal observers (from Fig. 2). Solid symbols are the amblyopic eyes (from Fig. 3); small open squares are the non amblyopic eyes. The amblyopic loss is always clearly greatest at small separations/eccentricities, and only two observers show a loss at the largest patch separation (CB and QM-Top). Reducing the contrast in the non-amblyopic eye to equate visibility accounts for some (but not all) of this loss (gray symbols).

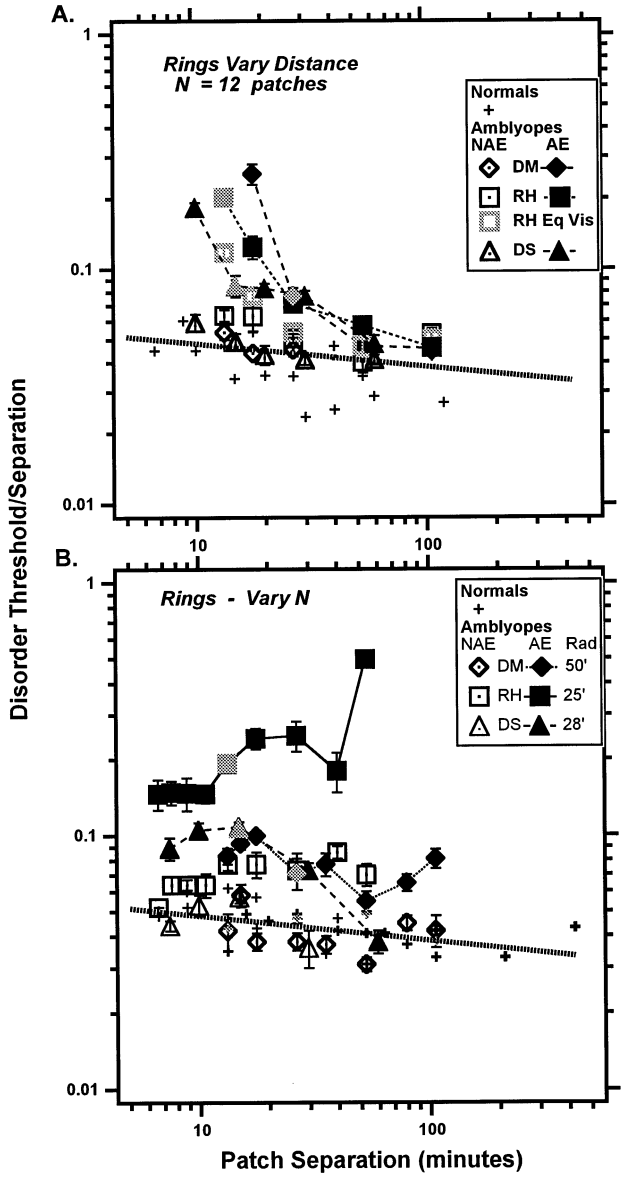

Fig. 8. Disorder detection thresholds for rings plotted as a Weber fraction of separation. (A) Varying distance ($N = 12$). Disorder detection thresholds (specified as a Weber fraction) of normal (crosses), amblyopic eyes (solid symbols) and non amblyopic eyes (open symbols) replotted from Fig. 5. (B) Varying N (the number of patches) while keeping the radius, patch size and spatial frequency constant. Varying the separation of the patches in a ring by varying N provides a direct test of the separation dependence of the amblyopic deficit with the patches at a fixed eccentricity (determined by the ring radius) and size. The large symbols show the data of the amblyopic eyes (solid symbols) and non-amblyopic eyes (open symbols) of three strabismic amblyopes. The small crosses show the data of the normal observers. The solid gray symbols in Fig. 8A,B (one for each of the three amblyopic eyes) represent identical stimulus conditions (i.e. $N = 12$, and the same radius, patch size and spatial frequency) measured in separate experiments (vary N and vary radius).

3.2.2. Equivalent intrinsic disorder (D_{eq}) in normal and amblyopic vision

In the normal fovea (open symbols Fig. 9), adding small amounts of external perturbation (base jitter) has

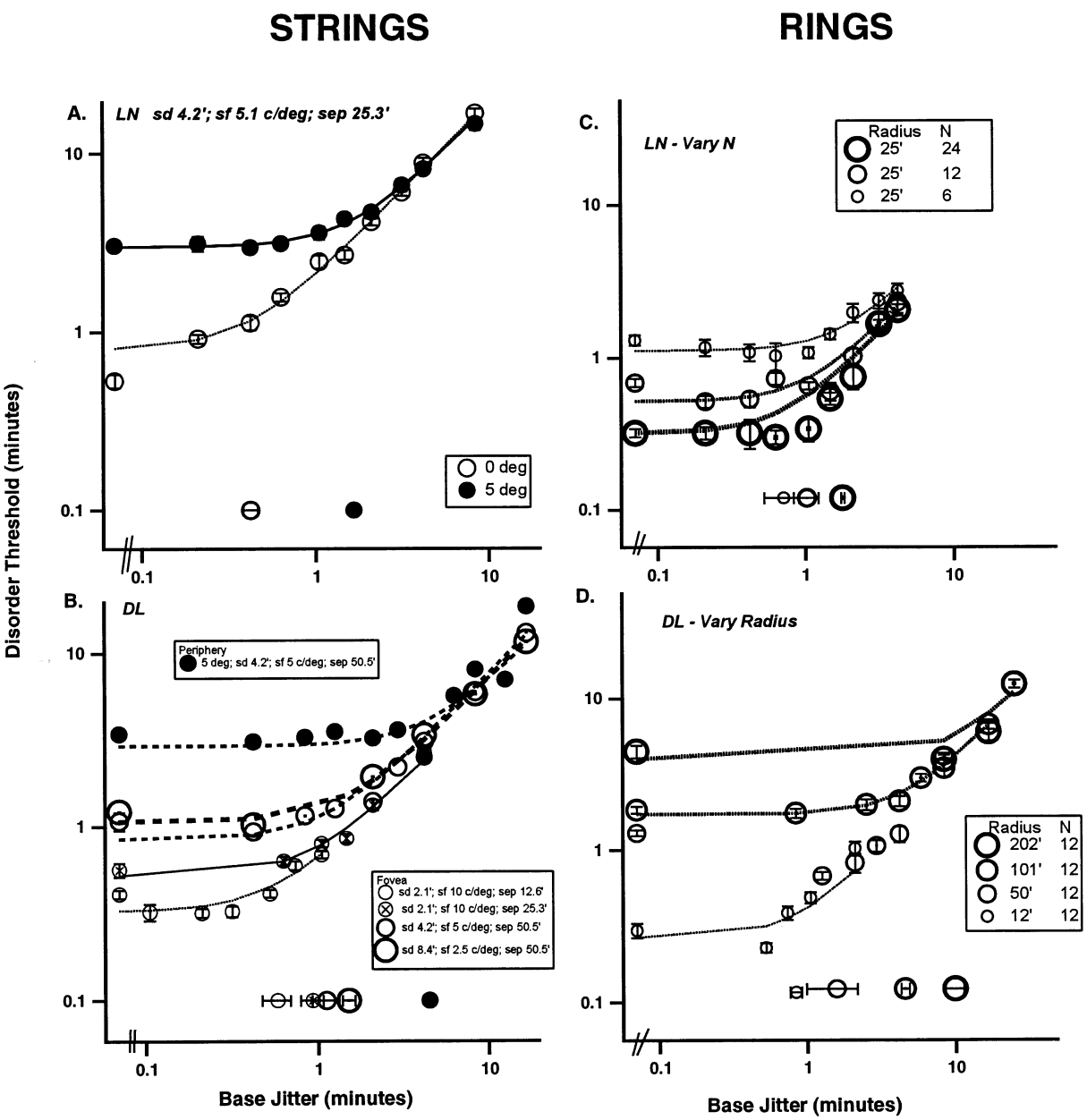

Fig. 9. Equivalent disorder for strings (A & B) and rings (C & D) in normal vision. Disorder discrimination thresholds are plotted as a function of the base external disorder (2-dimensional Gaussian jitter) in two normal observers. (A & B) Disorder discrimination thresholds for strings in the normal fovea (open symbols) and periphery (solid symbols). The lines fit to the data represent an equivalent noise function (see text), where the equivalent intrinsic disorder (D_{eq}) represents the horizontal position of the knee in the function and is represented by the symbols along the abscissa. For observer DL (B) foveal data are shown for a variety of stimulus conditions. Both the threshold with no external disorder (leftmost points) and D_{eq} depend on patch separation. Varying the size and spatial frequency of the patch at a fixed separation (the two largest open circles) has little effect. (C & D) Equivalent disorder for rings in normal vision. For LN (C), the circle radius, patch size and spatial frequency were held constant, and separation was varied by altering the number of patches spaced uniformly around the circle. For DL (D), the patch separation was altered by varying the viewing distance, which altered the circle radius as well as the patch size. Both of these manipulations lead to similar effects: both threshold in the absence of base jitter and D_{eq} are proportional to patch separation. The lines fit to the data represent an equivalent noise function (Eq. (3)).

little effect on disorder thresholds; however, as the base jitter increases, disorder thresholds increase in rough proportion to the base jitter. There are several points of interest in Fig. 9. First, for strings (Fig. 9A,B), both the thresholds at small values of base jitter, and D_{eq} (shown by the symbols plotted near the abscissa) are larger in peripheral (solid symbols) than foveal (open symbols) vision. Second, both Th_0 and D_{eq} depend on patch separation (see DL's foveal data in Fig. 9B and the summary data in Fig. 12). Third, varying the size and spatial frequency of the patch at a fixed separation has little (the two largest open circles in Fig. 9B) or no

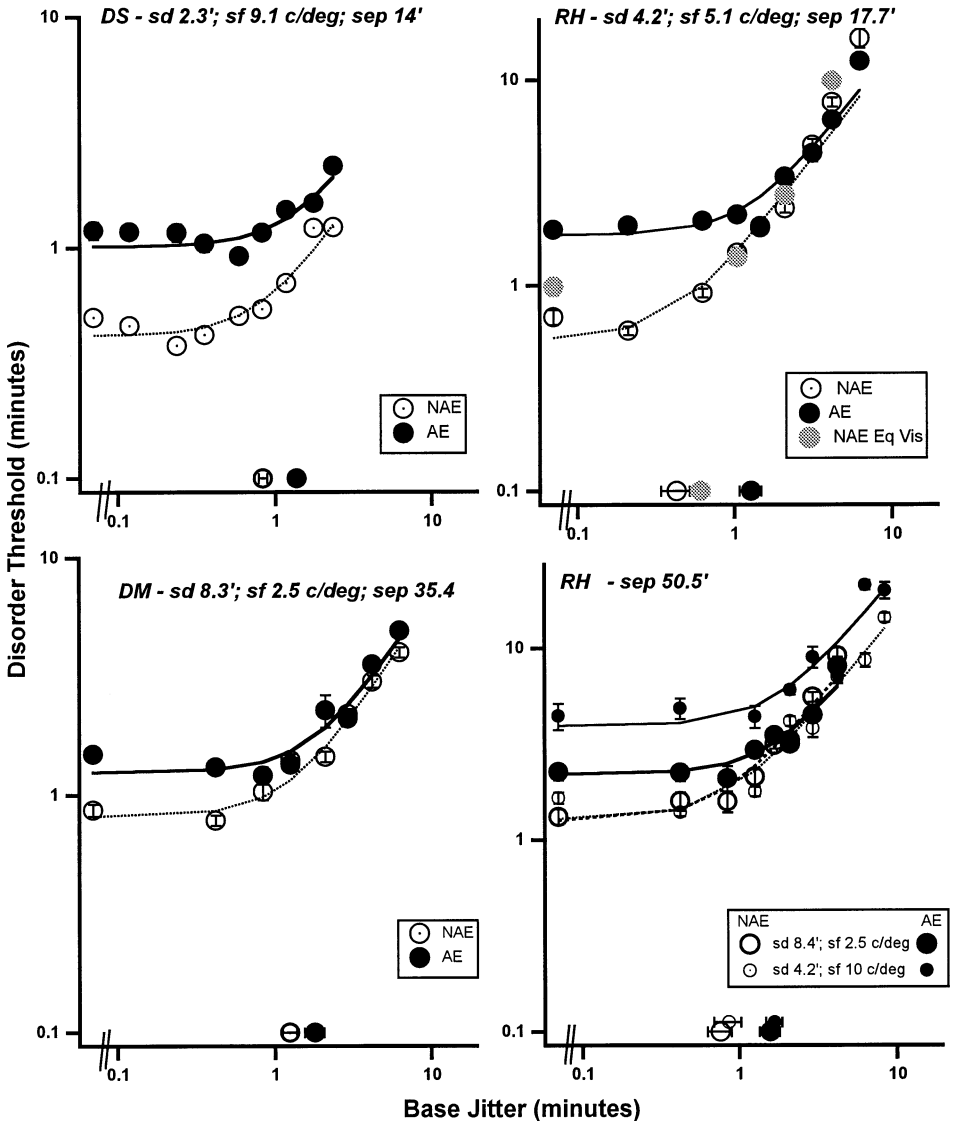

Fig. 10. Equivalent disorder for strings in amblyopic vision. Disorder discrimination thresholds for strings as a function of the base external disorder in the nonamblyopic (open symbols) and amblyopic (solid symbols) eyes of three observers with strabismic amblyopia. Amblyopic eyes show modest increases in disorder thresholds with no base jitter and equivalent disorder (D_{eq}). Lowering the contrast in the non-amblyopic eye (gray symbols top right panel) to equate the visibility increases thresholds and D_{eq} only slightly, and does not fully account for the effects of amblyopia. It is also interesting that while changing the patch size and spatial frequency (at a fixed separation) has a strong effect on disorder thresholds, it has almost no influence on D_{eq} in either eye (lower right panel).

(Fig. 10D) effect. Note that the curves shown in these Figures are the fits using Eq. (3). Eq. (1) gives identical fits, but the two equations are needed to give all the standard errors in Table 2.

The effect of separation can be seen more clearly with rings (Fig. 9C,D). For DL (Fig. 9D), the patch separation was altered by varying the viewing distance (which also altered the circle radius and patch size and spatial frequency). For LN (Fig. 9C), the circle radius, patch size and spatial frequency were held constant, and separation was varied by altering the number of patches spaced uniformly around the circle. Both of these manipulations lead to similar effects: both Th_0 and D_{eq} are nearly proportional to patch separation. These data are summarized by plotting them as a function of separation (open circles) in Fig. 13. It is interesting to note that while Th_0 and D_{eq} depend strongly on separation, efficiency seems to be independent of separation and N.

Amblyopic eyes show modest increases in disorder thresholds (Th_0) and equivalent disorder (D_{eq}) for both strings (Fig. 10) and rings (Fig. 11). Interestingly, the increased D_{eq} is not simply a result of reduced stimulus visibility in the amblyopic eye. Lowering the contrast in the non-amblyopic eye to equate the visibility in the two eyes increases thresholds and D_{eq} only slightly. It is also interesting that while changing the patch size and spatial frequency (at a fixed separation) has a strong

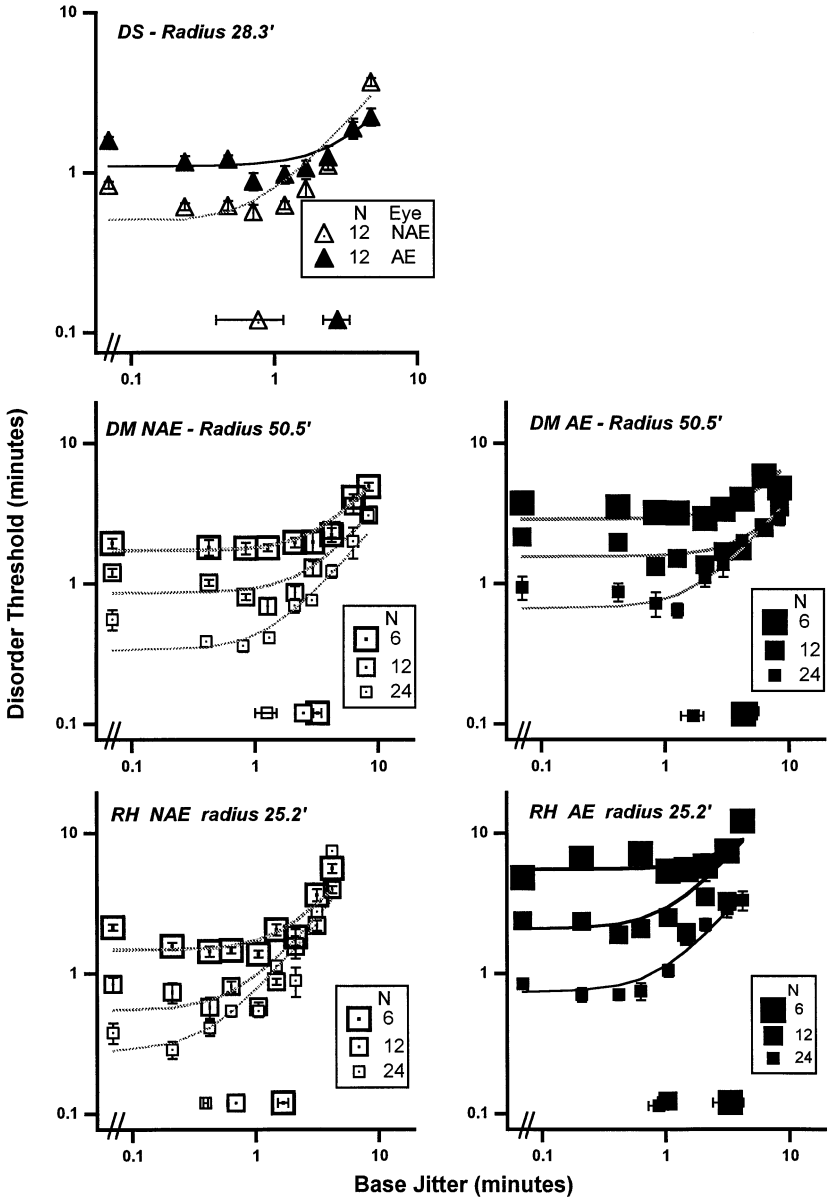

Fig. 11. Equivalent disorder for rings in amblyopic vision. Amblyopic eyes show modest increases in disorder thresholds in the absence of external jitter and equivalent disorder (D_{eq}) for rings. The strong effect of patch separation on both thresholds and on D_{eq} in both the non-amblyopic (open symbols) and amblyopic (solid symbols) eyes can be seen in the ring data with different numbers of patches (for DM and RH).

effect on disorder thresholds, it has almost no influence on D_{eq} in either eye (Fig. 10D). The strong effect of patch separation on both Th_0 and D_{eq} in the amblyopic eye can be seen in the ring data with different numbers of patches (Fig. 11), and in the summary data of Figs. 12 and 13. For a fixed patch separation both Th_0 and D_{eq} are increased in the amblyopic eye. This increased disorder can be mimicked in normal vision by increasing the separation between the patches in the string with N (the number of patches) fixed, or by decreasing N in the ring (and effectively increasing the separation between the patches). However, as we will show in the following section, adding real disorder to the stimuli does not mimic the increased equivalent disorder of the amblyopic eye.

3.2.3. Sampling efficiency (E)

Efficiency $[E = (N_{eff} - 1)/(N_{stim} - 1)]$ for both rings and strings is, on average, around 50% in normal vision (Table 2, and the bottom panels of Figs. 12 and 13). For strings the amblyopes show markedly reduced efficiency with their amblyopic eyes and several also show reduced efficiency with their preferred eyes, consistent with the data of Wang et al. (1998). Interestingly, two amblyopes also show less reduction of efficiency for rings.

Table 2
Equivalent noise and efficiency fit parameters

Task	Obs	Ecc	Sep	N	SD	SF	Th0	SE	E	SE	D_{eq}	SE
Strings	DL	0	12.60	5.00	2.10	10.00	0.33	0.03	0.62	0.16	0.56	0.08
Normal fovea	DL	0	25.30	5.00	2.10	10.00	0.52	0.05	0.64	0.09	0.93	0.14
	DL	0	50.50	5.00	4.20	5.10	0.90	0.07	0.44	0.05	1.12	0.20
	DL	0	50.50	5.00	8.30	2.50	1.07	0.06	0.40	0.04	1.51	0.13
	LN	0	25.30	5.00	4.20	5.10	0.62	0.06	0.24	0.01	0.68	0.35
	VS	0	28.40	5.00	4.70	4.50	0.41	0.06	0.60	0.07	0.72	0.11
	Mean											
Periphery	DL	5	50.50	5.00	4.20	5.10	2.91	0.38	0.48	0.05	4.49	0.30
	LN	5	25.30	5.00	4.20	5.10	2.61	0.06	0.45	0.01	3.93	0.48
	VS	5	28.40	5.00	4.70	4.50	1.80	0.18	0.67	0.14	3.47	0.45
	DL	10	50.50	5.00	8.30	2.50	4.83	0.42	0.54	0.07	7.90	0.67
	Mean											
Non amblyopic	RH	0	50.50	5.00	8.30	2.50	1.26	0.17	0.07	0.01	0.76	0.13
	RH	0	50.50	5.00	4.20	10.00	1.29	0.19	0.09	0.02	0.86	0.17
Eyes	RH	0	35.40	13.00	4.20	10.00	1.05	0.56	0.07	0.03	1.03	0.61
	RH	0	17.70	5.00	4.20	5.00	0.56	0.10	0.12	0.02	0.43	0.09
	RH EQ VISI	0	17.70	5.00	4.20	5.00	0.82	0.51	0.11	0.05	0.61	0.08
	DS	0	14.10	5.00	2.30	9.10	0.41	0.01	0.80	0.06	0.83	0.05
	DM	0	35.40	5.00	8.30	2.50	0.81	0.05	0.47	0.05	1.25	0.13
Mean												
Amblyopic eyes	RH	0	50.50	5.00	8.30	2.50	2.21	0.17	0.10	0.02	1.57	0.23
	RH	0	50.50	5.00	4.20	10.00	3.94	0.99	0.04	0.01	1.67	0.20
	RH	0	35.40	13.00	4.20	10.00	3.05	0.61	0.05	0.02	1.80	0.26
	RH	0	17.70	5.00	4.20	5.00	1.76	0.16	0.10	0.02	1.28	0.20
	DS	0	14.10	5.00	2.30	9.10	1.01	0.04	0.27	0.02	1.37	0.10
	DM	0	35.40	5.00	8.30	2.50	1.25	0.10	0.41	0.08	1.80	0.26
	QM	0	37.80	5.00	6.30	6.80	2.66	0.12	0.23	0.02	2.86	0.23
	Mean											
Rings	DL	3.37[a]	105.8	12	16.8	1.27	3.28	1.1	0.58	0.3	9.92	1.38
Normal fovea	DL	1.68	52.9	12	8.4	2.54	1.78	0.07	0.60	0.06	4.56	0.291
	DL	0.84	26.4	12	4.2	5.1	0.79	0.23	0.72	0.52	1.58	0.596
	DL	0.21	6.54	12	2.1	10.2	0.196	0.07	0.55	0.27	0.838	0.077
	LN	0.42	26.4	6	2.1	10.2	1.11	0.07	0.47	0.11	1.78	0.188
	LN	0.42	13.2	12	2.1	10.2	0.57	0.05	0.57	0.21	1.02	0.192
	LN	0.42	6.6	24	2.1	10.2	0.29	0.04	0.26	0.06	0.705	0.046
	Mean											
Non amblyopic eyes	RH	0.42	26.4	6	2.1	10.2	1.47	0.16	0.22	0.12	1.67	0.16
	RH	0.42	13.2	12	2.1	10.2	0.49	0.18	0.25	0.1	0.69	0.28
	RH	0.42	6.6	24	2.1	10.2	0.26	0.13	0.08	0.02	0.391	0.042
	DM	0.84	52.9	6	4.2	5.1	1.72	0.09	0.59	0.08	3.22	0.249
	DM	0.84	26.4	12	4.2	5.1	0.86	0.09	0.70	0.37	2.48	0.256
	DM	0.84	13.2	24	4.2	5.1	0.34	0.04	0.58	0.11	1.25	0.247
	DS	0.47	29.7	6	2.4	9.1	1.13	0.13	0.17	0.02	1.14	0.172
	DS	0.47	14.85	12	2.4	9.1	0.6	0.08	0.43	0.18	0.77	0.38
	Mean											
Amblyopic eyes	RH	0.42	26.4	6	2.1	10.2	5.48	0.45	0.05	0.02	3.31	0.907
	RH	0.42	13.2	12	2.1	10.2	2.01	0.41	0.05	0.02	1.04	0.179
	RH	0.42	6.6	24	2.1	10.2	0.71	0.06	0.05	0.01	0.879	0.157
	DM	0.84	52.9	6	4.2	5.1	2.86	0.21	0.38	0.09	4.3	0.483
	DM	0.84	26.4	12	4.2	5.1	1.62	0.13	1.43	1.23	4.7	0.962
	DM	0.84	13.2	24	4.2	5.1	0.67	0.1	0.27	0.04	1.7	0.345
	DS	0.47	14.85	12	2.4	9.1	1.2	0.1	0.73	0.55	2.77	0.58
	Mean											

[a] For rings ECC is equal to the ring radius.

3.2.4. The effect of N on detecting disorder

If performance were limited by topographical jitter (noise), increasing the number of samples (patches) should improve thresholds for detecting disorder. Indeed, an ideal observer model (Levi & Klein, 1986; Wang et al., 1998) predicts that thresholds should improve by $\sqrt{(N-1)}$ for disorder detection and this is precisely what happens when disorder thresholds are

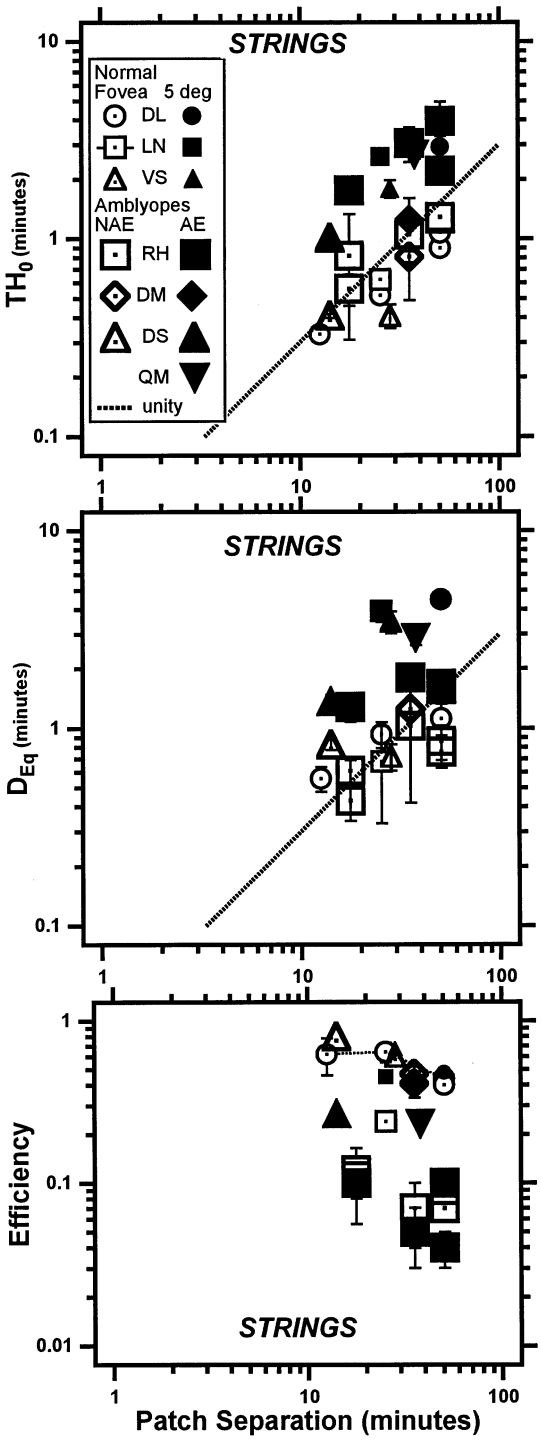

Fig. 12. Summary of Th_0 (top panel), D_{eq} (middle panel) and efficiency (bottom panel) for strings. Th_0, D_{eq} and efficiency were obtained from the equivalent noise fits to all the string data (Fig. 9A,BFig. 10 plus some data not shown previously). Th_0 and D_{eq} are more or less proportional to patch separation (the dotted line has a slope of 1). For a fixed patch separation both Th_0 and D_{eq} are increased in the amblyopic eye (solid triangles) compared to the normal fovea (○) or non-amblyopic (△) eyes. Both Th_0 and D_{eq} are also increased in peripheral vision (at 5° — ●).

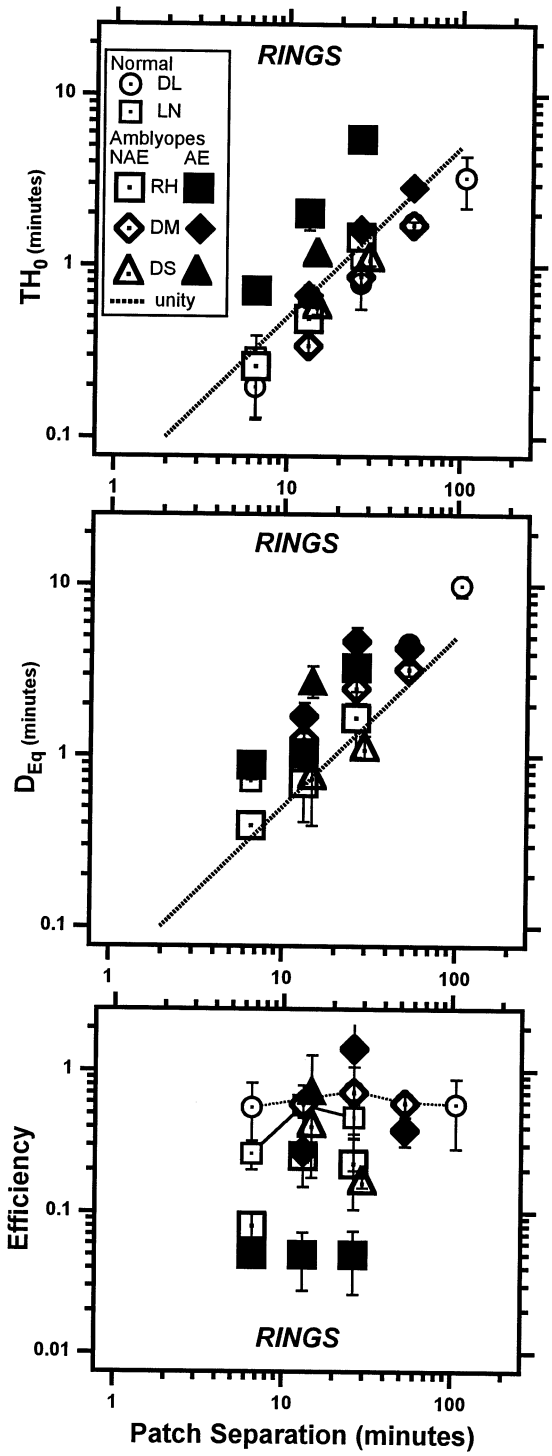

Fig. 13. Summary of Th_0 (top panel), D_{eq} (middle panel) and efficiency (bottom panel) for rings. Both Th_0 and D_{eq} obtained from the equivalent noise fits (Eqs. (1) and (3)) to all the ring data (Fig. 9C,DFig. 11) are more or less proportional to patch separation (the dotted line has a slope of 1). For a fixed patch separation both Th_0 and D_{eq} are increased in the amblyopic eye (solid triangles) compared to the normal fovea (small open symbols) or non-amblyopic (large open symbols) eyes.

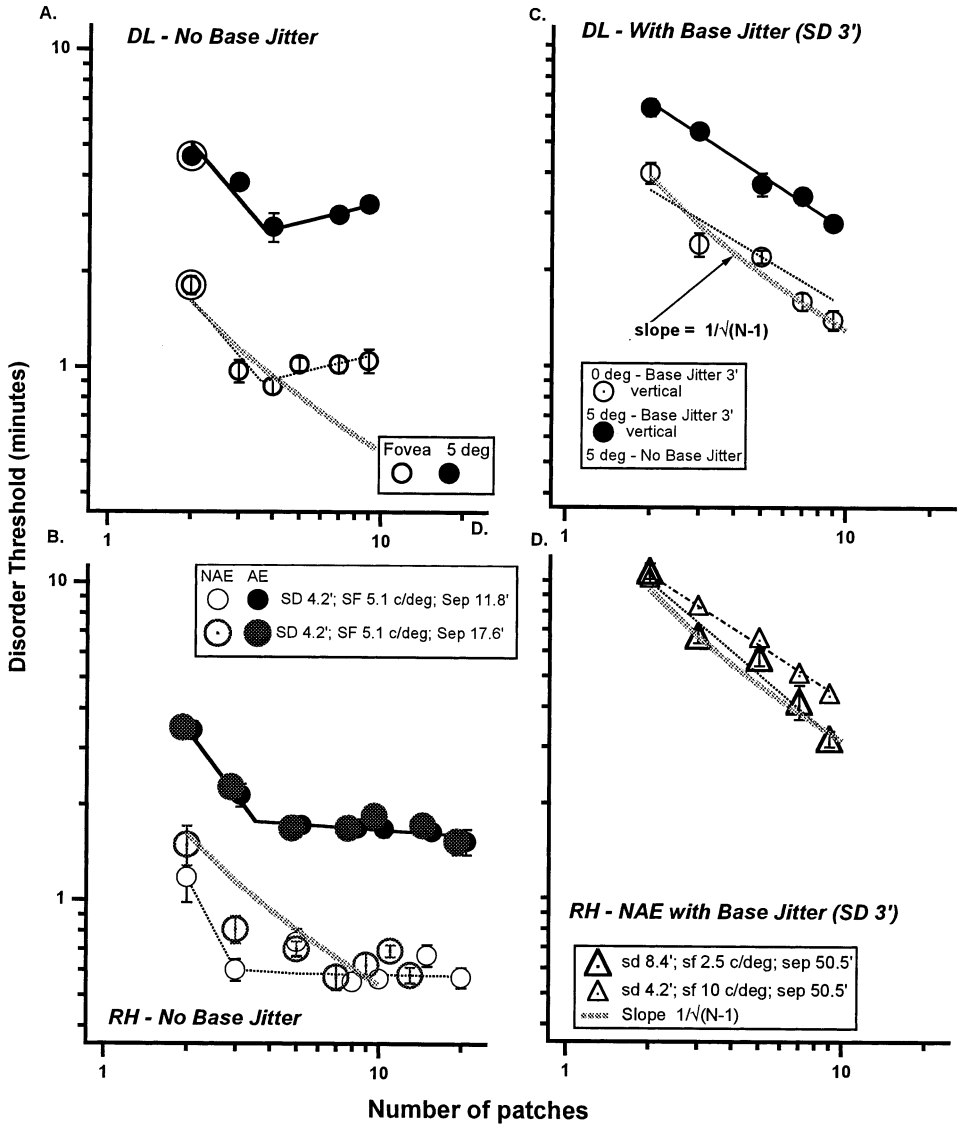

Fig. 14. The effect of N (the number of patches) on disorder thresholds for strings. Left panels: Disorder detection thresholds improve rapidly (slope ≈ -1.0) when N increases from 2 (left most points — which are 'encircled' in A) to about 4, and do not decrease further (in fact they may actually increase slightly) with further increases in N. This plateau suggests a floor that limits performance that can not be reduced by averaging or integrating the positions of multiple samples. Data are shown for a normal observer (DL – top left) viewing foveally (open symbols) or at 5° (solid symbols) and for the non-amblyopic (open symbols) and amblyopic (solid symbols) eye of a strabismic amblyope (RH — lower left). Right panels: Disorder detection thresholds in the presence of high (3′) external base jitter. When disorder thresholds are measured for strings varying in N in the presence of added external noise, both the normal fovea (open symbols — top right) and periphery (solid symbols — top right) and the non-amblyopic eye (open symbols — lower right) of a strabismic amblyope (RH) show thresholds improving by approximately $\sqrt{(N-1)}$ (as indicated by the thick dotted line).

measured for strings varying in N in the presence of added external noise (standard deviation = 3′; Fig. 14C,D). However, the square root dependence on N is not evident in the normal fovea or periphery or in either eye of the strabismic amblyopes in the absence of added external jitter (Fig. 14A,B). Disorder thresholds improve rapidly (slope ≈ -1.0) as N increases from 2 to about 4, and do not decrease further (in fact they may actually increase slightly) with further increases in N. This plateau suggests a floor that limits performance that can not be reduced by averaging or integrating the positions of multiple samples. Note that the floor for the zero jitter case (left panels) is lower than the data for the right panels.

As noted previously, the square root dependence on N is not found for rings either when there is no external disorder. Increasing N while keeping the radius constant results in a proportional decrease in thresholds ($\approx$ constant Weber fraction) for both normal and amblyopic (Fig. 8B) eyes. Increasing N in a ring of fixed radius, proportionally reduces the patch separation, which strongly constrains performance (Levi & Klein, 2000).

4. Discussion

Our goal was to evaluate the sensitivity of the human visual system (both normal and amblyopic) to spatial disorder, and to ask whether there is increased 'intrinsic' topographical disorder in the amblyopic visual system. We found that in normal foveal vision, sensitivity to spatial disorder is strongly dependent on the separation between the patches. For rings, thresholds are around 3–4% of the patch separation (Weber fractions of 0.03–0.04); for strings thresholds are even better (Weber fractions of ≈ 0.02), once the separation exceeds about 20–30 arcmin.

4.1. Limiting factors in shape perception in normal vision

It is now clear that there are multiple factors that limit spatial vision and shape perception. There is considerable evidence that both eccentricity and separation dependent processes can limit spatial judgements (e.g. Levi & Klein, 1990c; Whitaker & Latham, 1997). The eccentricity dependent ('local sign') process is extremely precise. Under ideal conditions, thresholds may be as low as 0.67% of the target eccentricity (Klein & Levi, 1987; Levi & Klein, 1990c). The high precision for detecting disorder in strings, when the separation of the patches is greater than about 30′ (thresholds $\approx 1/70$ of the eccentricity of the limiting patches for separation/eccentricity $> 30'$) is consistent with an eccentricity dependent process (Levi & Klein, 1990c; Levi & Tripathy, 1996; Whitaker & Latham, 1997). However, this eccentricity limited mechanism appears to be delicate, and is degraded when the stimulus features are not aligned. On the other hand, the separation dependent process is less precise, but appears to be more robust (for a discussion see Morgan & Watt, 1989; Levi & Klein, 1990c). Our present results suggest that in normal vision, detection of disorder in rings is limited by a separation dependent process, since performance depends on patch separation, when eccentricity is fixed (vary N experiments). Several mechanisms have been proposed for this separation dependent process, including second-stage filters (Burbeck & Hadden, 1993), coincidence detectors (Morgan & Regan, 1987), and counting a fixed number of neural units between features (Hirsch & Hylton, 1982). A full discussion of the mechanisms underlying Weber's law is beyond the scope of this paper. However, it is clear from Figs. 8 and 9 that the normal Weber relationship is severely compromised in the amblyopic visual system.

4.2. Limiting factors in shape perception in strabismic amblyopia

Amblyopic eyes show decreased sensitivity to disorder, particularly when the patches are closely spaced and have relatively high spatial frequencies. An equivalent noise analysis suggests that equivalent disorder (D_{eq} — the amount of disorder that must be added to the stimulus to increase thresholds by $\sqrt{2}$) is higher in the amblyopic eye. In addition, we found that amblyopic eyes showed reduced efficiency (particularly for strings), consistent with the results of Wang et al. (1998). However, we argue below that the strong separation dependence of Th_0 and D_{eq} are not consistent with increased intrinsic topographical disorder limiting pattern perception in amblyopia.

Topographical disorder could, in principle, take a number of forms. For example, if the standard deviation of receptive field positions of the amblyopic eye were increased by a fixed amount relative to those of the normal eye, this would add a fixed amount of intrinsic disorder. For example, if this extra scatter of receptive field positions were 1mm, the added intrinsic disorder would be approximately 3 arc min in the fovea (assuming a cortical magnification factor of 20 mm/deg in the fovea), regardless of the spatial scale of analysis. We will refer to this form of topographical disorder as the 'fixed scatter' model. An alternative model of receptive field scatter is the scale-invariant model described by Hess and Holliday (1992), in which the disorder is a fixed fraction of the receptive field size. In this model, the intrinsic disorder would depend on the spatial scale of analysis. Neither of these models can easily accommodate our results.

We found that disorder thresholds and D_{eq} depend strongly on patch separation (Figs. 12 and 13). Moreover, changing the patch size and spatial frequency has little influence on D_{eq} in either the amblyopic or preferred eye (Fig. 10D). Both the fixed scatter and the scale-invariant models can predict the effect of separation in strings, if disorder (scatter) increases with eccentricity. Specifically, if we assume that performance is limited primarily by the precision with which the patches on either side of the central patch can be localized, then, increasing the separation in a string would increase the eccentricity of the limiting patches. Indeed, this is the basis of the eccentricity model shown in Fig. 2 (Levi & Tripathy, 1996). However, neither the fixed scatter nor the scale-invariant models can predict the effect of separation (obtained by varying N) in rings, since varying N (at a fixed radius) alters only the separation, but does not alter either the patch size and spatial frequency or the eccentricity. Thus, we conclude that neither of the simple models of topographical disorder can account for all of our results. Moreover, as noted above, neither the normal nor the amblyopic visual systems use N (the number of patches) efficiently to improve performance in detecting disorder in strings, as predicted by an ideal observer model, or by adding

(external) disorder to the stimuli (see Fig. 14). Thus, amblyopia cannot be mimicked by simply adding disorder to the stimuli. Below we examine an alternative hypothesis.

Detection of disorder requires several steps: the observer must detect and localize each patch, calculate its position relative to its neighbors, and compare the positions of the samples with an internal representation of a perfectly ordered pattern. Topographical disorder would limit the ability to precisely localize each patch unless the position of each receptive field were 'known' at a higher level of processing. Thus, the notion of uncalibrated disorder (as discussed in Section 1) has received a good deal of attention. However, the separation dependence of both thresholds and D_{eq} (when the scale and eccentricity of the stimuli are fixed) suggest that the limitation for detecting disorder may lie in comparing the positions of the samples relative to its neighbors,[2] whether this is accomplished by a second stage filter or by counting the number of intervening neural units (Hirsch & Hylton, 1982). If this assumption is correct, then the 'intrinsic' error that limits detection of disorder in strabismic amblyopia may be an abnormality in the comparison process that leads to Weber's law. What we are suggesting is that rather than the positions of cortical receptive fields being either improperly calibrated (or uncalibrated) in the amblyopic brain, it is separation or distance that is improperly calibrated. In this respect, the amblyopic eye acts like a normal eye with the samples more widely separated (see Figs. 12 and 13). Both Th_0 and D_{eq} are increased in the amblyopic eye. This increased disorder can be mimicked in normal vision by increasing the separation between the patches in the string with N fixed, or by decreasing N in the ring (and effectively increasing the separation between the patches). The analysis above suggests that the main factor limiting disorder detection by amblyopes is separation dependent, i.e. a 'Weber' noise. Since this Weber noise is intrinsic, it can be argued that it reflects a separation dependent (rather then a stimulus size dependent) intrinsic disorder. In all likelihood, both size and separation dependent noise can limit performance (and probably do under different stimulus conditions, cf. Demanins & Hess, 1996); however, under our testing conditions, the separation dependent process appears to limit performance.

Note that we are not arguing against the notion of increased topographical error in the amblyopic visual system (or that increased jitter would influence the Weber fraction). Rather we are arguing that two aspect of our data cannot easily be accounted for on the basis of topography: (1) the separation dependence of D_{eq} when stimulus eccentricity and size are fixed; and (2) the saturation of disorder thresholds when N is increased (Fig. 14).

Why does the amblyopic eye act like a normal eye with the sample spacing increased? We speculate that the patches are sparsely represented in the visual cortex of strabismic amblyopes, at the level of pattern analysis. This is consistent with several recent studies showing that strabismic amblyopes do not use all the samples of a pattern efficiently for Vernier acuity (Wang et al., 1998) or pattern discrimination (Levi et al., 1999). Moreover, strabismic amblyopes systematically underestimate the number of samples with their amblyopic eye, even when the samples are visible and clearly resolved (Sharma, Levi & Klein, 2000). Although there is evidence consistent with undersampling at a post-receptoral stage (Sharma, Levi & Coletta, 1999), the sparse representation may occur at a level beyond V1. For example, a recent functional imaging study (PET) in human amblyopes found a selective reduction of activation in Brodmann areas 18 and 19 when the visibility of the patterns was equated in the amblyopic and non-amblyopic eyes (Imamura, Richter, Fischer, Lennerstrand, Franzen, Rydberg et al., 1997).

4.3. Relationship to other studies

Separation places important limitations on performance in other tasks too. For example, the well known Weber relationship between separation and threshold holds for a wide range of position tasks, including bisection, Vernier alignment, etc. (Sullivan, Oatley & Sutherland, 1972; Klein & Levi, 1987; Levi & Klein, 1990c; Morgan & Watt, 1989). Moreover, it has recently been reported that the deficit in 3-patch alignment in the amblyopic eye depends upon both patch size and separation (Demanins and Hess, 1998). It is of interest to note that their stimuli were vertically separated Gabor patches in which the (vertical) carrier grating was orthogonal to the (horizontal) offset, so that for small separations (they used separations as small as 2σ) the carrier may have provided useful cues to the offset.

Our results with rings (or sampled circles) are closely related to recent studies of sensitivity to distortions in continuous circles (Wilkinson, Wilson & Habak, 1998; Hess et al., 1999). Wilkinson et al. (1998) used continuous, rather then sampled circles, and argued for a global computation in which contour information is pooled relative to the center of an object. Our sampled stimuli and data can be related to the continuous case by considering our samples as being at the extrema of an oscillating sinusoid. For example, a Fourier shape descriptor with three cycles going around the circle, would be expected to have thresholds similar to our

[2] Comparing the positions of the samples with an internal representation of a perfectly ordered pattern should not depend on the number of samples.

sampled case with $N = 6$, where the samples are placed at the peaks and troughs of the grating. Our results are not consistent with a simple pooling operation, since we can trade off the amount of contour information (N) with radius. Rather, the strong dependence on sample separation, suggests that performance in our task may be limited by low level inputs to the higher level mechanisms involved in global shape analysis.

Previous work (Flom, Bedell & Barbeito, 1986; Sireteanu, Lagreze & Constantinescu, 1993) also suggests that strabismic amblyopes demonstrate large perceptual errors (biases) in judging the locations of samples around a circle. Strabismic amblyopes also show poor performance in discerning distortions in continuous circles (Pointer & Watt, 1987; Hess et al., 1999). Pointer and Watt (1987) used continuous circles defined by lines. Since their stimuli were broadband, poor performance by the amblyopic eye might have been due to shifts in the spatial scale of analysis. More recently, Hess et al. (1999) used continuous circular band-pass targets (D4s). They also found that strabismic amblyopes were less sensitive at detecting deformations (sinusoidal) from circularity with the amblyopic eye. Neither their results nor ours can be explained by stimulus visibility or by shifts in spatial scale. Hess et al. argue that their results are not a consequence of undersampling because the loss was: (1) present at all scales; and (2) additive (i.e. the amblyopic and preferred eye's discrimination curves converge at high levels of external base jitter). Let us consider these two points.

Both our results and Hess's show that the amblyopic deficit increases with spatial frequency (our Fig. 6 and Hess et al.'s Fig. 5), even when stimulus visibility is taken into account. For example, DM shows an approximately 7-fold loss at 10 c/deg, compared to a less than 2-fold loss at 5 c/deg. Moreover, neither DM nor RH were able to perform the task with their amblyopic eyes at spatial frequencies above 10 c/deg. This spatial frequency dependence is not consistent with a scale invariant topographical jitter model. While the spatial frequency dependence would be expected on the basis of undersampling, both observers show modest losses at 5 c/deg, well below their resolution limit.

Both our results and Hess's show that the amblyopic deficit is additive (i.e. in Figs. 10 and 11 the AE and NAE converge at high jitter. This would imply that there is not much loss of efficiency in the amblyopic compared to the non amblyopic eye. Note, however, that for some amblyopes (particularly RH, both eyes are degraded (Figs. 13 and 14). We speculate that the additive nature of the loss might be early and discriminates between the AE and NAE. However, the loss of efficiency in the two eyes may be late (possibly extrastriate) and therefore more independent of eye of origin. Extrastriate cortex may have gotten confused by the input from the amblyopic eye, and not developed normally, resulting in a loss of efficiency in both eyes. Note that this loss of efficiency in the non amblyopic eye was also evident in the study of Wang et al. (1998). Hess et al. (1999) attribute the additive nature of the deficit to increased topographical disorder (neural disarray); however, our results (e.g. Figs. 13 and 14) show that the equivalent 'intrinsic' disorder depends on the separation between the samples. While we agree with Hess et al. (1999) that the additive error is consistent with increased intrinsic noise, this result is not easily attributable to alterations in topography, since in our 'vary N' experiments with rings, the eccentricity of the samples remained fixed. Rather, we suggest that the 'intrinsic' error that limits detection of disorder in strabismic amblyopia may be an abnormality in the comparison process that leads to Weber's law, because the patches are sparsely represented in the visual cortex of strabismic amblyopes, at the level of pattern analysis. Note that we are not arguing that there is no additional topographical disorder in the amblyopic visual system. In the limit, there may be a raised level of disorder. However, in our view there is little evidence to support the notion that there is widespread uncalibrated neural disarray occurring at all spatial scales. Rather, we are arguing that distance or position may be miscalibrated, because the signals are unreliable (or absent) when viewing with the amblyopic eye.

To summarize, we evaluated the sensitivity of the human visual system (both normal and amblyopic) to spatial disorder. We found that in normal foveal vision, sensitivity to spatial disorder is strongly dependent on the separation between the patches. Amblyopic eyes show decreased sensitivity to spatial disorder, and increased equivalent disorder (D_{eq}). However,the strong separation dependence of Th_0 and D_{eq} for rings is not consistent with increased intrinsic topographical disorder limiting pattern perception in amblyopia. Rather, we suggest that the 'intrinsic' error that limits detection of disorder in strabismic amblyopia may be an abnormality in the comparison process that leads to Weber's law, because the patches are sparsely represented in the visual cortex of strabismic amblyopes, at the level of pattern analysis.

Acknowledgements

We are grateful to Hope Queener for programming these experiments. This research was supported by Research grants R01EY01728 and RO1 EY04776, a Core Center Grant P30EY07551, and short-term training grant T35EY07088 from the National Eye Institute This research was supported by grants R01EY01728 and P30EY07551 from the National Eye Institute, NIH, Bethesda, MD.

Appendix A

This Appendix considers two items: (1) The connection between the task of detecting a displacement when the direction is known (i.e. bisection or alignment) to the task when it is unknown (present paper). (2) The question of why in our task the ideal observer's accuracy improves as $1/\sqrt{(N-1)}$ rather than $1/\sqrt{(N-2)}$.

A.1. Part 1

It is useful to connect the disorder thresholds of the present paper to the bisection and Vernier thresholds of many of our earlier papers. For simplicity we will analyze the three-dot case where the outer dots are fixed and the middle dot is shifted. We will call our earlier work the direction-known case and the present work the direction-unknown case. For the direction-known case (Vernier or bisection) our rating scale response uses categories from -2 to $+2$ to indicate the direction of shift. For the direction-unknown case (related to the energy model) the rating scale response uses categories from 0 to $+4$ to indicate the magnitude of the shift away from the bisection point, where the shift can be in any two dimensional direction (Levi & Klein, 2000).

The connection between the direction-known (i.e. 1-dimensional) and direction-unknown (i.e. 2-dimensional) shifted dot, is identical to another situation that has been well examined in the field of audition: the ideal observer's performance for detecting a phase known versus a phase unknown sinusoid (Peterson, Birdsall & Fox, 1954; Jeffress, 1964; Green & Swets, 1966). One can draw criteria lines, in two-dimensional 'phasor' space, that separate the different stimuli. For the phase known case the criteria separating the categories are straight lines. For the phase unknown case the criteria are circles. For the phase known case the transducer function relating d' to stimulus strength is linear. For the phase unknown case the transducer function is a quadratic at low contrast and rapidly becomes a straight line at higher contrast. For $d' > 1.5$ the transducer function is quite straight.

Klein and Carney (1996) and Klein (in preparation) have approximated the shape of the phase-unknown transducer function using several analytic functions. We will translate Klein's results to the present case by replacing the word 'phase' with the word 'direction'. A simple function that does an excellent job of matching the direction-unknown transducer is a power function below threshold and a straight line above threshold as given by:

$$d' = (c/\mathrm{Th})^n \qquad \text{for } c \le \mathrm{Th} \tag{A1}$$

and

$$d' = 1 + n(c/\mathrm{Th}) - n \qquad \text{for } c \ge \mathrm{Th} \tag{A2}$$

where c is the stimulus strength (the offset in the present case), $n = 1.78$ is the exponent that provides a good fit to the true transducer function and Th is the detection threshold that gives $d' = 1$. This function has an rms error of 0.015 d' units between d' of 0 and 3 when compared to the true ideal observer function. It is useful to compare the direction-known and direction-unknown cases. For offsets above threshold the direction-unknown transducer is well approximated by the direction-known transducer shifted downward in d' units by an amount ranging between 0.6 and 0.73. The direction-unknown threshold is 1.73 times larger than the direction-known threshold. Thus if Weber fractions of 0.010 are found for the direction-known case (Klein & Levi, 1987) then we would expect thresholds of 0.017 for the disorder case of the present paper. Human performance may be slightly more degraded (by about $\sqrt{2}$) because human observers cannot attend to two dimensions simultaneously and maintain high precision (Jiang & Levi, 1991). When there are more than three dots, as in our present experiments the analysis is more complicated, but we would expect similar results. The multidot case is now taken up as the second part of this Appendix.

A.2. Part 2

Consider first the three-line bisection task of Wang et al. (1998). The central line was a solid line. The outer two lines consisted of separated dots with random spacing and with each sample given a random jitter. Suppose there were eight samples in each of the outer lines. The ideal observer would calculate the average location of all 16 outer dots and compare the result to the location of the middle line. Suppose the middle line's position is known exactly since it is a solid line with no random jitter (in our paper we do add a small uncertainty for this line but for simplicity we omit that here). The ideal observer prediction for the bisection threshold would be $\sigma/\sqrt{(N)}$ where σ is the standard deviation of the position of each dot, and $N = 16$ is the total number of samples. $N = 16$ since each dot is independent and contributes to the averaging process.

For the disorder judgment of the present experiments the situation is different because we do not have a fixed reference corresponding to the central line of the Wang et al. (1998) experiments. Consider the one-dimensional task of N dots on a horizontal line with the location of each dot jittered in the horizontal direction. One can estimate the disorder by first calculating the difference in location of adjacent dots (there will be $\mathrm{Np} = N - 1$ pairs) and then calculating the variance of the distances. The variance will be calculated based on two difference assumptions:

Assumption 1. There is no prior information about the average separation between dots. In that case the variance (called var1) is:

$$\text{var1} = \sum (d_i - d_{\text{ave}})^2/(\text{Np} - 1) \quad \text{(A3)}$$

$$\text{var1} = \sum = (d_i - d_{\text{ave}})^2/(N - 2) \quad \text{(A4)}$$

where d_{ave} is the average interval, averaged over the Np samples. The factor of $\text{Np} - 1$ in Eq. (A3) is the standard variance factor produced by the fact that only $\text{Np} - 1$ of the deviations, $d_i - d_{\text{ave}}$, are independent since these deviations have zero mean.

Assumption 2. Suppose the experiment consists of many trials and the average separation is fixed across all the runs. In that case, the observer could memorize the average separation and the variance is given by:

$$\text{var2} = \sum (d_i - d_{\text{mem}})^2/(\text{Np}) \quad \text{(A5)}$$

$$\text{var2} = \sum (d_i - d_{\text{mem}})^2/(N - 1) \quad \text{(A6)}$$

where d_{mem} is the memorized separation. In this case the variance decreases with N according to $1/(N - 1)$ rather than the $1/(N - 2)$ factor that occurs when the memory cue is not present. This reasoning applies to the 2-dimensional case of the present paper.

In our experiments the average separation was held fixed across trials, so a memory cue is possible. For that reason we have adopted the more conservative $1/(N - 1)$ factor. We call this the more conservative option since it produces a lower ideal observer prediction and therefore a reduced human efficiency. Note that the data in Fig. 14 with external jitter (right column) is reasonably well fit by this assumption.

References

Barlow, H. B. (1956). Retinal noise and absolute threshold. *Journal of the Optical Society of America*, *46*, 634–639.

Bradley, A., & Freeman, R. D. (1981). Contrast sensitivity in anisometropic amblyopia. *Investigative Ophthalmology and Visual Science*, *21*, 467–476.

Burbeck, C. A., & Hadden, S. (1993). Scaled position integration areas: accounting for Weber's law for separation. *Journal of the Optical Society of America*, *A*, *10*, 5–15.

Demanins, R., & Hess, R. F. (1996). Positional loss in strabismic amblyopia — interrelationship of alignment threshold, bias, spatial scale and eccentricity. *Vision Research*, *36*, 2771–2794.

Field, D. J., & Hess, R. F. (1996). Uncalibrated distortions vs undersampling. *Vision Research*, *36*, 2121–2124.

Flom, M. C., Bedell, H. E., & Barbeito, R. (1986). Spatial mechanisms for visual acuity deficits in strabismic and anisometropic amblyopia-developmental failure or adaptation? In E. L. Keller, & D. S. Zee, *Adaptive processes in visual and oculomotor systems* (pp. 45–51). New York: Pergamon Press.

Green, D. M., & Swets, J. A. (1966). *Signal detection theory and psychophysics*. Wiley.

Hess, R. F., & Holliday, I. E. (1992). The spatial localization deficit in amblyopia. *Vision Research*, *32*, 1319–1339.

Hess, R. F., & Field, D. (1993). Is the increased spatial uncertainty in the normal periphery due to spatial undersampling or uncalibrated disarray? *Vision Research*, *33*, 2663–2670.

Hess, R. F., & Field, D. (1994). Is the spatial deficit in strabismic amblyopia due to loss of cells or an uncalibrated disarray of cells? *Vision Research*, *34*, 3397–3406.

Hess, R. F., & Howell, E. R. (1977). The threshold contrast sensitivity function in strabismic amblyopia: evidence for a two-type classification. *Vision Research*, *17*, 1049–1055.

Hess, R. F., Campbell, F. W., & Greenhalgh, T. (1978). On the nature of the neural abnormality in human amblyopia: neural aberrations and neural sensitivity loss. *Pflugers Archives*, *377*, 201–207.

Hess, R. F., McIlhagga, W., & Field, D. J. (1997). Contour integration in strabismic amblyopia: the sufficiency of an explanation based on positional uncertainty. *Vision Research*, *37*, 3145–3161.

Hess, R. F., Wang, Y. Z., Demanins, R., Wilkinson, F., & Wilson, H. R. (1999). A deficit in strabismic amblyopia for global shape detection. *Vision Research*, *39*, 901–914.

Hirsch, J., & Hylton, R. (1982). Limits of spatial frequency discrimination as evidence of neural interpolation. *Journal of the Optical Society of America*, *72*, 1367–1374.

Imamura, K., Richter, H., Fischer, H., Lennerstrand, G., Franzen, O., Rydberg, A., Andersson, J., Schneider, H., Onoe, H., Watanabe, Y., & Langstrom, B. (1997). Reduced activity in the extrastriate visual cortex of individuals with strabismic amblyopia. *Neuroscience Letters*, *225*, 173–176.

Jeffress, L. A. (1964). Stimulus-oriented approach to detection. *Journal of the Acoustic Society of America*, *36*, 766–774.

Jiang, B. C., & Levi, D. M. (1991). Spatial-interval discrimination in two-dimensions. *Vision Research*, *31*, 1931–1937.

Keeble, D. R. T., & Hess, R. F. (1999). Discriminating local continuity in curved figures. *Vision Research*, *39*, 3287–3299.

Kiorpes, L., Kiper, D. C., & Movshon, J. A. (1994). The effect of blur and positional jitter on Vernier acuity in normal and amblyopic macaque monkeys. *Ophthalmology and Visual Science* (*Supplement*), *35*, 2064.

Klein, S. A., & Levi, D. M. (1987). The position sense of the peripheral retina. *Journal of the Optical Society of America*, *A*, *4*, 1543–1553.

Klein, S. A., & Carney, T. (1996). Transducer function for energy (viewprint) models. *Society for Information Display* 96 *Digest*, *27*, 425–428.

Levi, D. M., & Harwerth, R. S. (1977). Spatio-temporal interactions in anisometropic and strabismic amblyopia. *Investigative Ophthalmology and Visual Science*, *16*, 90–95.

Levi, D. M., & Klein, S. (1985). Vernier acuity, crowding and amblyopia. *Vision Research*, *25*, 979–991.

Levi, D. M., & Klein, S. A. (1986). Sampling in spatial vision. *Nature*, *320*, 360–362.

Levi, D. M., & Klein, S. A. (1990a). Equivalent intrinsic blur in spatial vision. *Vision Research*, *30*, 1971–1993.

Levi, D. M., & Klein, S. A. (1990b). Equivalent intrinsic blur in amblyopia. *Vision Research*, *30*, 1995–2022.

Levi, D. M., & Klein, S. A. (1990c). The role of separation and eccentricity in encoding position. *Vision Research*, *30*, 557–585.

Levi, D. M., & Klein, S. A. (1996). Limitations on position coding imposed by undersampling and univariance. *Vision Research*, *36*, 2111–2120.

Levi, D. M., & Tripathy, S. P. (1996). Localization of a peripheral patch: the role of blur and spatial frequency. *Vision Research*, *36*, 3785–3803.

Levi, D. M., & Klein, S. A. (2000). Seeing Circles: What limits shape perception? *Vision Research*, *40*, 2329–2339.

Levi, D. M., Klein, S. A., & Aitsebaomo, A. P. (1985). Vernier acuity, crowding and cortical magnification. *Vision Research*, *25*, 963–977.

Levi, D. M., Sharma, V., & Klein, S. A. (1997). Feature integration in pattern perception. *Proceedings of the National Academy of Sciences USA*, *94*, 11742–11746.

Levi, D. M., Waugh, S. J., & Beard, B. L. (1994). Spatial scale shifts in amblyopia. *Vision Research*, *34*, 3315–3334.

Levi, D. M., Klein, S. A., & Sharma, V. (1999). Position jitter and undersampling in pattern perception. *Vision Research*, *39*, 445–465.

Morgan, M. J., & Regan, D. (1987). Opponent model for line interval discrimination: interval and vernier performance compared. *Vision Research*, *27*, 107–118.

Morgan, M. J. M., & Watt, R. J. (1989). The Weber relationship for position is not an artefact of eccentricity. *Vision Research*, *29*, 1457–1463.

Pointer, J. S., & Watt, R. J. (1987). Shape recognition in amblyopia. *Vision Research*, *27*, 651–660.

Pelli, D. G. (1990). The quantum efficiency of vision. In C. Blakemore, *Visual coding and efficiency*. Cambridge: Cambridge University Press.

Peterson, W. W., Birdsall, T. G., & Fox, W. C. (1954). The theory of signal detectability. *IRE Transformation and Information Theory*, *4*, 171–212.

Sireteanu, R., Lagreze, W. D., & Constantinescu, D. H. (1993). Distortions in two-dimensional visual space perception in strabismic observers. *Vision Research*, *33*, 677–690.

Sharma, V., Levi, D.M., & Klein, S.A. (2000). Undercounting features and missing features: evidence for a high-level deficit in strabismic amblyopia. *Nature Neuroscience* (in press).

Sharma, V., Levi, D. M., & Coletta, N. J. (1999). Sparse-sampling of gratings in the visual cortex of strabismic amblyopes. *Vision Research*, *39*, 3526–3536.

Sullivan, G. O., Oatley, K., & Sutherland, N. S. (1972). Vernier acuity as affected by target length and separation. *Perception and Psychophysics*, *12*, 438–444.

Wang, H., Levi, D. M., & Klein, S. A. (1998). Spatial uncertainty and sampling efficiency in amblyopic position acuity. *Vision Research*, *38*, 1239–1251.

Watt, R. J., & Hess, R. F. (1987). Spatial information and uncertainty in anisometropic amblyopia. *Vision Research*, *27*, 661–674.

Watt, R. J., Ward, R. M., & Casco, C. (1987). The detection of deviation from straightness in lines. *Vision Research*, *27*, 1659–1678.

Whitaker, D., & Latham, K. (1997). Disentangling the role of spatial scale, separation and eccentricity in Weber's law for position. *Vision Research*, *37*, 515–524.

Wilkinson, F., Wilson, H., & Habak, C. (1998). Detection and recognition of radial frequency patterns. *Vision Research*, *38*, 3555–3568.

Wilson, H. R. (1991). Model of peripheral and amblyopic hyperacuity. *Vision Research*, *31*, 967–982.

Zeevi, Y. Y., & Mangoubi, S. S. (1984). Vernier acuity with noisy lines: estimation of relative positional uncertainty. *Biological Cybernetics*, *50*, 371–376.